Current status on plastic scintillators modifications

Guillaume H.V. Bertrand, Matthieu Hamel, Fabien Sguerra

▶ **To cite this version:**

Guillaume H.V. Bertrand, Matthieu Hamel, Fabien Sguerra. Current status on plastic scintillators modifications. Chemistry - A European Journal, 2014, 20, pp.15660 - 15685. 10.1002/chem.201404093 . cea-01827633

HAL Id: cea-01827633

https://cea.hal.science/cea-01827633v1

Submitted on 4 Apr 2023

HAL is a multi-disciplinary open access archive for the deposit and dissemination of scientific research documents, whether they are published or not. The documents may come from teaching and research institutions in France or abroad, or from public or private research centers.

L'archive ouverte pluridisciplinaire **HAL**, est destinée au dépôt et à la diffusion de documents scientifiques de niveau recherche, publiés ou non, émanant des établissements d'enseignement et de recherche français ou étrangers, des laboratoires publics ou privés.

Current status on plastic scintillators modifications

*Guillaume V.H. Bertrand, Fabien Sguerra and Matthieu Hamel**

CEA, LIST, Laboratoire Capteurs et Architectures Électroniques, F-91191 Gif-sur-Yvette Cedex, France.
E-mail: matthieu.hamel@cea.fr

Keywords: Plastic scintillators, polymers, fluorescence, dyes, nuclear instrumentation, radiation detector.

Abstract : Recent developments of plastic scintillators are reviewed, from 2000 to present, distributed in two different chapters. First chapter deals with the chemical modifications of the polymer backbone, whereas modifications of the fluorescent probe are presented in the second chapter. All examples are provided with the scope of detection of various radiation particles. The main characteristics of these newly created scintillators and their detection properties are given.

1. Introduction

Protections of civilians and facilities against CBRN-E (Chemical, Biological, Radiological, Nuclear, and Explosives) threats represent a true challenge due to the constant increase of world's population movements. According to Dr. El Baradei (1997 – 2009 IAEA Director General), terrorists who are unconcerned about exposing themselves to radiation could easily conceal a source in a truck or a suitcase. *"The danger of handling powerful radioactive sources can no longer be seen as an effective deterrent, which dramatically changes previous assumptions. […] Security of nuclear and other radioactive material has taken on dramatically heightened [in IAEA's work] significance in recent years."*

As an example, a dramatic story happened in late 2013 in Mexico, where a radioactive cobalt-60 source (3000 Curies, 111 TBq) was stolen from its transportation truck. Fortunately, the material was safely recovered 8 days later.[1]

In this context, numerous detectors could be used for NR detection. Among them, we will focus in this Review on plastic scintillators (hereafter abbreviated as PS[1]). These materials can be defined as one or several fluorescent probes embedded in a polymer matrix. For instance, a typical scintillation cocktail is made from *p*-terphenyl and POPOP dissolved in polystyrene. To detect Special Nuclear Materials, plastic scintillators present several advantages. They are cheap (especially interesting for large size detection systems), sensitive to gamma rays, can be handled without any specification, reliable, stable and can be prepared in large volumes. More particularly, the choice of the detector will become extremely important in the future due to the combination of the cheapness of PS ($ 2,000 for a 3.8 cm × 36 cm × 173 cm large PVT detector, compared to $ 6,000 for a 5 cm × 10 cm × 41 cm NaI(Tl) inorganic scintillator[2]) and the necessity for some countries to cover at the best their borders with radiation portal monitors. But some drawbacks have incited several groups to renew with chemical developments of plastic scintillators: they display a poor resolution, were presumed for a long time to be unable to perform fast neutron/gamma discrimination, afford relative low scintillation yields compared with inorganic scintillators and cannot give access to the full energy of an incident gamma.

As explained before, plastic scintillators were first described in the late 50's. Chemically, a PS is composed of a polymer matrix, usually fluorescent, hosting one or several fluorescent molecules (Figure 1). The basic principle of radiation/matter interaction is as follows: when an impinging radiation interacts with the polymer, it will lose a given part of its energy, depending on its nature. Alpha particles which are highly ionizing but heavy will thus interact

[1] Standard abbreviations used in this document: α-NPO: 2-(1-Naphthyl)-5-phenyloxazole; BBO: 2,5-bis-(4-biphenylyl)-1,3,4-oxadiazole; CL: Cathodoluminescence; CQD: carbon quantum dot; DVB: dinvinylbenzene; FOM: Figure Of Merit; IBIL: Ion Beam Induced Luminescence; LiMA: Lithium Methacrylate; Li-Sal: Lithium Salicylate; MEH-PPV: Poly[2-methoxy-5-(2-ethylhexyloxy)-1,4-phenylene-vinylene; MPA : Mercaptopropionic acid; MOF: Metal Organic Framework; NMP: 1-methyl-2-pyrrolidinone; PBBO: 2-(4-biphenylyl)-6-phenylbenzoxazole; PBD: 2-(4-Biphenylyl)-5-phenyl-1,3,4-oxadiazole; PEG: poly(ethylene glycol); PL: Photoluminescence; PBMA: Poly(benzyl methacrylate); PMMA: Poly(methyl methacrylate); POPOP: 1,4-Bis(5-phenyl-2-oxazolyl)benzene; PPO: 2,5-Diphenyloxazole; PS: Plastic scintillator; PSD: Pulse shape discrimination; PSt: polystyrene; PVA: Polyvinyl alcohol; PVK: Polyvinylcarbazole; PVT: Polyvinyltoluene; QD: Quantum dots; SEM: Scanning electron microscopy; SSD: Spectral shape discrimination; St: styrene, TTA: Triplet triplet annihilation.

within a few micrometers (e.g. an alpha of energy 5 MeV will penetrate within 35 µm). Contrarily, a 1 MeV gamma would need not less than 14 cm and a 1 MeV electron 4.3 mm to release their energy. As explained, since the mean free path will be different for each particle, the response of the plastic scintillator should vary with them. Actually, this is not often the case, as for instance it was assumed for a long time that neutron and gamma rays were not distinguishable due to their neutral nature.

So, when energy is deposited inside the plastic scintillator, multiple interactions occur, and among others, the matrix will allow the release of UV photons. Following other interactions, emerging photons will be transferred from UV to visible light where it will be recovered with photodetectors, such as photomultiplier tubes (Figure 2). This photon-electron conversion will allow physicists to give access to the radiation/matter interaction.

Depending on their application, plastic scintillators display both advantages and drawbacks. On one hand, they are cheap, available in large dimensions and morphologies, doped with various elements, have a large choice of emission wavelengths and have a fast response. On the other hand, their light response is moderate (light yield of typically 10,000 ph per MeV of deposited energy), have a low density and effective atomic number, so are not efficient for gamma spectroscopy and display a poor resolution.

We will see in this Review that chemical modifications of these materials can lead to differentiations in the particles' responses.

To this aim, the goal of this Review is to define new developments of plastic scintillators. Despite the fact that many tools of detection devices have been improved (electronics, signal processing, etc.), most of commercial PS are those which were developed in the 50's[3] and the 60's. This Review will be limited to developments from 2000 to march 2014, unless particularly relevant data were published before this date. The reader can refer to other reviews in this field for previous improvements.[4,5] This Review will discuss mainly about chemical developments, and is thus less oriented to the nuclear physics point of view, even if

application examples are given when available. It is therefore structurally-based on chemical developments (first part about the modification of the polymer; second part about the modification of the fluorescent probe). However, as the goal is devoted to nuclear detection, materials will also be described in terms of characteristics such as scintillation yield (or light output), decay time, scintillation wavelength, and so on. Also, pictures of plastic scintillators are given when available. Sometimes some publications deserve to be classified in several topics (e. g. metal loading of a specially designed polymer). They will be therefore referenced two or several times.

Also, this Review is exclusively limited to plastic scintillators and derivatives (composites, sol-gel, etc.). No data will be given regarding improvements on organic single crystals, optical (scintillating) fibbers, liquid scintillators and inorganic scintillators.

2. Modification of polymer for special applications

2.1. PMMA-Based scintillators

Poly(methyl methacrylate) (PMMA) occupied a special place in the transparent plastic for scintillation family. A review especially devoted to that topic was recently published by Salimgareeva and Kolesov.[6] This review makes a very precise and complete overview of PMMA-based scintillator technology before 2005. We strongly recommend this publication as a complement of this part as we will focus on post-2005 developments.

Unlike polystyrenes, polysiloxanes or polyepoxides cited in this review, PMMA does not have any benzene rings in its backbone. Hence, it lacks of primary emitters but in returns confers a very high near UV transparency. This compromise makes him a target of choice for scintillation application as the monomer methyl methacrylate (MMA) is quite cheap and its polymerization chemistry well known (Scheme 1). In Polystyrene-based plastic scintillators the energy deposited by an ionizing radiation is mainly absorbed by the polymer matrix, which can be efficiently transferred to the emitters *via* Förster energy exchange,[7] whereas

PMMA-based scintillators will have to rely on less efficient non-radiative exchanges. Primary emitters are frequently referred as the secondary solvent because they have to account for a great part of the scintillator to maximize scintillation yield. Most of the past century works were performed using naphthalene[8] used as primary emitter. Classical characteristics of a PMMA-based scintillator are: scintillation yield ≈ 5,000 ph/MeV (which means the number of photons created after the deposition of 1 MeV from the particle), decay time ≈ 3 ns, typical sample size 3 cm^3. But early 2000's research showed that it can be replaced by 1,1,3-trimethyl-phenylindan[9] as a reliable solution to achieve up to 12,000 ph/MeV scintillation yields. Different mixtures of secondary and tertiary emitters have been tried with success,[10] and once again all of this has been exhaustively described in Salimgareeva's review.

More recently Van Loef *et al*. evaluated the use of PBMA [Poly(benzyl methacrylate)] for fast neutron/gamma discrimination purpose but pulse height experiments revealed very low scintillation yield (< 1,000 ph/MeV). They also conclude that PVT and PSt equivalents are more suited and give good result for the design application. [11]

PMMA is also characterized by a refractive index which strongly differs than the Polystyrene one; this property has been used for cladding scintillating plastic fibbers.[12]

2.2. Polysiloxanes

Polysiloxanes were an early subject of study for scintillation applications.[13] They differ to traditional plastic scintillators as they are elastomer and often referred as silicon rubber. Their main attractive feature is their very flexible chain, which gives them a wide range of temperature stability[14] and irradiation tolerance. Polysiloxanes were early identified as a seducing alternative to PSt or PVT-based plastic sensors as they proved to be five to ten times more resistant to radiation (rad-hard). This has been explained in the early 2000, with chain's flexibility as the main argument. It was stated that upon ionizing condition, radicals from chains homolitically cut can recombine or react without damaging the backbone nor impeding on the physical characteristic at doses up to 3.5 MGy.[15]

Polysiloxane is a rather vague naming as it defines a large family, but for scintillation application it is widely admit that cross-linked copolymers containing phenyl groups are the system of choice. On a synthetic standpoint, this system is composed of vinyl terminated diphenylsiloxane-dimethylsiloxane copolymer (resin A) and hydride terminated methylhydrosiloxane-phenylmethylsiloxane copolymer (resin B) (Scheme 2). The rubber is synthesized using a platinum catalyzed hydrosilylation. Karstedt's catalyst enables room temperature vulcanization of the resins mix. Different ratio of diphenylsilyl in resin A have been explored, however a ratio superior to 22 % have dramatic consequences on the sample's transparency (transmission < 75 %). Classical characteristics of a Polysiloxane based scintillator are: scintillation yields ≈ 3,000 to 6,000 ph/MeV, decay times ≈ 5 ns, typical sample size 2 cm^3.

The main drawback of this family of polymer is the poor solubility of the major fluorescent dyes. For instance PPO loading is always in the range 1 - 1.5 %.[16] It has been shown that the fluorescence quenching due to aggregation counteracts the increase of PPO concentration. In the same study by Quaranta *et al.*,[17] it was also proved that the phenyl emission intensity arising from the polysiloxane core decreases as PPO concentration increases (Figure 3). This is a strong clue as how excited states transfer from the backbone to the primary dye; hence the percentage of phenyl rings in the copolymer structure will have an impact on the scintillation yields. And this has been recently highlighted[17c] with a work that describes optical and scintillation response of polysiloxanes with various phenyl contents synthesized using a blend of resin A and modified resin B to overcome the 22 % limit previously stated. The designed polymers did not give the expected result of increasing emission intensity with increasing quantity of phenyl groups in the blend. But it did point out the increase of phenyl-phenyl excimer formation as the number of phenyls goes up. We can also note that higher quantity of phenyl decreases the stability of the device toward high doses. Another drawback for silicon rubber / PPO matrices is that they are more absorbent in the near UV than their PSt and PVT

counterparts. This issue can be partially bypassed by adding a red emitter to the mix which gives a 17 % increase of the collected light when coupled with an appropriate photomultiplier (Figure 4).[17d] This last work also shows the capability of polysiloxane-based scintillators to achieve satisfying neutron detection.

The low solubility of classic luminescent dyes in polysiloxane copolymer also forbade to access good intrinsic neutron/gamma detection through high concentration technic (see corresponding chapter), but it is possible to engineer this type of plastic scintillator for neutron detection To tackle this topic research has been focused on incorporating, in polysiloxane matrix, elements with high neutron cross section, such as Boron or Gadolinium.[16a] Gadolinium doping was briefly studied by Bell *et al*., who successfully incorporated tri-nitro or tris(tri-butylphosphate)gadolinium complexes in polysiloxane. Unfortunately they observed a lesser light output (≈ 50 %) than the PVT equivalent.

Loading with Boron has been more researched for thermal neutron detection thematic. *Closo*-carborane cages linked to base resins are used to achieve high boron loading, it was observed that *ortho* and *para* carboranes are less stable than the *meta* one.[16a] In most of the reported compositions Boron concentration oscillates around 2 to 5 wt%, except one report where a plastic scintillator device was prepared with up to 18 % by weight of Boron.[18] The high nuclear cross section for neutron absorption and its low atomic number make Boron a candidate for neutron/gamma discrimination, although the presence of Si atoms in the matrix is known to make polysiloxane sensitive toward gamma ionization by Z_{eff} increase. On a pure detection aspect Boron loading in polysiloxane gave the same performance as the commercial PVT counterpart.[19] It was also demonstrated that the boron loading had no effect on the internal quantum efficiency (no quenching of dye's excited states) but slightly inhibited energy transfers from the matrix to the dyes[20] (decrease of the light output when the loading increases).

Commenté [MH2133201]:
Décrire la synthèse ?

FS : Ils n'en parlent pas dans le papier.

2.3. Epoxy resins

Polyepoxydes, most commonly epoxy or araldite, are a class of materials that cover a wide range of applications due to their easy chemical tuning. It is not surprising to get transparent and easy-to-cast polyepoxyde matrix containing fluorophores for scintillation purpose. All epoxy resins share the same practical use: they are good glue and readily polymerize at room temperature. That is why the main application of epoxy in radio detection is not as a scintillator matrix but as optical glue.[21] Polyepoxydes are obtained by mixing two components: a prepolymer, the "binder" and a curing agent, also called "hardener". These two molecules, once mixed, give a highly cross-linked network (Scheme 3). Classical characteristics of an epoxy based scintillator are: scintillation yields reported around ≈ 50% of Pilot B scintillator, decay times ≈ 10 ns, typical sample size 3 cm^3.

Most of the recent work was done with a commercial optical epoxy[22] (EpoTek™ 305) which seems to be very close to standard epoxy glues. Early interest in the 60's quickly showed major limitation: a very low UV transmission (Figure 5), and poor solubility of classic scintillating molecules.[23] Recent experiments have nonetheless use polyepoxyde as a matrix because of its easy handling that does not need any chemistry knowledge. Encapsulation of inorganic fluor BaF_2:Ce was attempted[24] following step of early 90's technology.[25] 50 nm crystals were successfully and homogeneously trapped in the matrix after curing. The good refractive index match between the polymer and BaF_2:Ce was not sufficient to compensate the loss of transmitted light through the sample. Despite being obviously designed for radiation detection no data are available concerning their use under ionizing radiation. Another recent study[26] used polyepoxyde to, as they claimed, create long lifetime luminescent organic dye embedded in an organic matrix. Their objective is to use long decay pulse in a plastic scintillator/optical fiber/detector set up to differentiate pulse from the plastic and pulse from stray ionization of the fiber. They choose polyepoxyde for the purpose of immobilizing xanthene dyes in a transparent matrix. The authors of this paper claimed this immobilization

will promote phosphorescence by decreasing vibrational or O_2 quenching of triplet states and thus enable the observation of long luminescence lifetime (0.7 to 3.0 ms). Nor real proof of this effect is reported neither clear count vs. channel graph to support this theory. Luminescence lifetime data were given without graphic showing time resolution of luminescence vs. wavelength which cast serious doubt about the attribution of the phosphorescence peak.

2.4. Polyesters

Polyethylene terephthalate (PET)[27] and polyethylene naphthalate (PEN)[28] have been proven to be radioluminescent without the addition of any fluorophores. PET scintillation yield is rather modest (2,200 ph/MeV) but higher scintillation output is claimed for its naphthalene counterpart (10,500 ph/MeV). Nevertheless PEN radioluminescence intensity seems to vary drastically with the polymer quality and the surface treatment of the samples.[29] Furthermore PEN and PET degradation is observed under laser and proton beam.[30] Loading a PEN matrix with ^{6}LiF in order to achieve thermal neutron detection has been performed,[31] but the samples suffer from low transparency, even for 150 µm thicknesses, due to a lack of solubility of ^{6}LiF in the polymer matrix, which is the opposite of the detection system goal (large system are required for light detection efficiency).

2.5. Polyimides

Carturan and Quaranta have extensively studied the use of polyimides for scintillation purpose. [32] Polyimide films are typically prepared from 4,4'-hexafluoroisopropylidenediphthalic anhydride / diaminobenzophenone solution in NMP, this solution being further doped with different amounts of Rhodamine B, spin coating on silica plates and curing at various, elevated temperature (Scheme 5). The formed polyimide is able to fluoresce and acts as a photon donor to Rhodamine B. Upon irradiation with 5.478 MeV

alpha particles, these films displayed a scintillation efficiency of about 14 %, *i. e.* 1,400 ph/MeV relative to NE-102 plastic scintillator (equivalent to BC-400 PS).

To this study was added Nile Red as dye dopant and these films were later studied by Ion Beam Induced Luminescence (IBIL).[33] The samples were irradiated by 2.0 MeV $^{4}He^{+}$ ion beam at fluences ranging between 10^{12} and 10^{15} ions/cm^{2}. IBIL results indicated that the polyimide-based scintillator has better radiation hardness and good scintillation efficiency for high doses irradiations. In their last report,[33c] three different fluorinated polyimides were prepared and compared towards radiation hardness. With all these improvements, efficiencies ranging from 50 to 60 % relative to NE-102 have been reached (5,000 – 6,000 ph/MeV). To the best of our knowledge, this was the first use of rhodamine B as dye for scintillation purpose.

2.6. Loading with elements

2.6.1. Metal loading

The wide diversity of polymer matrices for scintillation applications enables a variety of possible chemistry. Among it, inorganic chemistry is particularly attractive as it gives complementary solution to a large range of scintillation thematic (Table 1). We can differentiate two main ideas behind the use of metals in plastic scintillator: the increase of density to increase gamma interaction with radiation, or target a nucleus known to have a large cross section towards a specific radiation type.

Commenté [MH2133202]: Phrase à reformuler

2.6.2. Lithium, Boron, Cadmium and Gadolinium loadings for thermal neutron detection

Commenté [MH2133203]:
Classer le paragraphe dans l'ordre :
-Li
-B
-Gd
Ou peu importe, car c'est un peu le fouillis.
Je n'ai pas vu le cadmium

The desired isotopes with large cross section toward neutron are given in Table 2 with their natural abundances.

As it can be seen all along this paper, recent focus has been made on neutron detection, and PMMA-based scintillators bring some solutions to the table. As we can see in the chapter dealing with metal loading, absorption of thermal neutrons by a plastic scintillator can be a

true challenge. In order to increase nuclear cross section towards neutron, the monomer can be engineered to include Lithium-6 atom (Figure 6a).[34] Lithium-6 is a naturally occurring isotope (7.5 wt%) but a recent study showed that it was possible to synthesize (enriched) Lithium methacrylate (LiMA 95 wt%).[35] Both natural and enriched LiMAs were successfully copolymerized with styrene up to a 1:10 ratio respectively. As expected the enriched LiMA gave better performance toward thermal neutron detection (Figure 6b, Figure 7).

Britvich *et al.*[65] reported the use of neutron absorbers for plastic scintillators loading, either in the form of *o*-carborane (4 %), boric acid[36] (3 %) or ^{6}LiF (0.1 %). Relative light yields compared with BC-404 are 82 %, 60 % and 90 %, respectively.

Another way to incorporate Lithium in plastic scintillators is to blend in inorganic crystal. This approach can be used to combine different interesting elements. A typical example is Lithium Gadolinium Borate doped with Cerium (LGB)[37, 38a] which makes scintillating microcrystals that can be blended in PVT matrix (BC-490), or a possible neutron spectrometry.[39] This work demonstrated an increased resolution on small sample (60 cm^3) for mono energetic proton beam, but also claimed that higher volumes do not increase the resolution[38b] due to the weak light output and the diffusive nature of the dispersed LGB.

Some work has also been performed on gadolinium loading in plastic fibers[40] without clear presentation of the chemical structure. Gadolinium loading in the form GdF_3 nanoparticles has also been reported.[41] Finally Lithium, Boron and Cadmium can also be introduced after the polymerization *via* extrusion technics. Nanoparticles are mixed with PSt or PVT pellets in an extruder to form a mix that can be cast.[42] This will be further developed in the appropriate section.

In the early 2000's researchers started to anticipate the shortage of ^{3}He which is used in discharge tubes for thermal neutron detection. An early alternative was to incorporate Boron in PSt and PVT matrices for scintillation application. Boron loaded scintillators could be sensitive to fast neutrons (recoil proton from neutron interaction) and thermal neutrons

(Boron-10, which after capture of a thermal neutron produces alpha and lithium particle). This duality pushed Normand *et al.* to synthesize and to characterize new formula in 2002.[43] The scintillator composition is a classical 1.5 wt% *p*-terphenyl, 0.01 wt% POPOP in styrene with 5 wt% of boron. No further formulation was available as the boron source is proprietary.

This work aimed at surpassing the performances of the commercial BC-454 plastic scintillator with four time cheaper material. They indeed showed the feasibility of thermal neutron/gamma discrimination[43a] and application to waste drum assessment (Figure 8).[43c] Boron can also be introduced *via* carborane compound in a polystyrene matrix. It has been shown that this method can also produce PS doped with 5 wt% of boron. This loading did not affect the light output (Figure 9) and gave a dramatic increase in thermal neutron detection (Figure 10).[44] On a side note this technology has been experimented for monitoring *in situ* neutron capture therapy.[45]

Gadolinium was also blend in a polymer matrix. Research struggle to overcome a loading over 0.5 wt%, but in 2001 the use of HMPA as an additive was found to increase the solubility of gadolinium nitrate[46] and gadolinium chloride[47] in methyl methacrylate and gave access to a plastic scintillator with up to 3 wt% loading of Gd. This loading decreased the light output (estimated at 5,000 photons/MeV) but increased the sensitivity toward neutron detection (Figure 11).[46] The same phenomenon was observed for gadolinium phenyl-carboxylate (Scheme 6a), phosphinate or phosphine derivatives were found to increase their solubility in styrene, and achieve loading as high as 5 wt% for a 60 % light yield of the unloaded PS.[48]

Organo-gadolinium compounds could also be used without additives to enhance the neutron cross section of PS; a first example was published in 2009 by Ovechkina *et al*. It described the use of gadolinium isopropoxide (Scheme 6b) blended in a polystyrene matrix up to, here again, 3 wt%. This materials show good characteristics (scintillation yields = 8,500 ph/MeV for a 3 wt% Gd loading) and some promising neutron response.[49] Unfortunately these first

results were not exploited to its full potential. Another analysis was performed on gadolinium phenylpropionate in styrene (Scheme 6c)[50] which only showed the negative influence of gadolinium doping on the light yield, no neutron response was reported.

A solution to reach higher Gadolinium loading was proposed recently by Payne *et al*.[51] They achieved very high metal loading using functionalized Gd_2O_3 nanocrystals to create a nanocomposite with up to 40 wt% of capped Gd_2O_3 (which correspond to a 22.7 wt% loading of Gd). On the one hand, this high Gd incorporation decreased significantly the transmission of the device, but it also enabled the observation of a photoelectric peak under 662 keV gamma irradiation (Figure 12). We can note here that this study does not mention thermal neutron detection even if they have high Gd loading.

To the best of our knowledge, only a single publication refers to the use of 2-vinylnaphthalene, doped with lithium as monomer for PS.[52] The preparation of poly(2-vinylnaphthalene) is not described. Loaded with 6-lithium salicylate (Li-Sal) as neutron capture reagent and fluorophore (λ_{max}^{em} = 408 nm), it enables the detection of thermal neutrons. Li-Sal was readily prepared from the reaction between salicylic acid and ^{6}LiOH in acetone / water at 60°C (Scheme 7). Thin film samples (thickness 110 µm) doped with 25 % of LiSal were thus obtained and exposed to radiation flux. The Authors mentioned that unloaded poly(2-vinylnaphthalene) revealed to be insensitive to neutrons or gamma. Unfortunately the material seems opaque even at low thickness (Figure 13).

A recent extension of this work consisted in biaxially stretching PEN films for thermal neutron detection.[53] Large scale (≈ 1 m^2), ^{6}LiF loaded films were successfully prepared. Biaxially stretched composite poly(ethylene naphthalate) had 20 % higher neutron light yield as compared to unstretched composite film.

Another use of lithium salicylate was described by Mabe *et al*. Transparent lithiated polymer films were obtained from another new matrix: poly(styrene-*co*-lithium maleate) (alternating ratio 1:1).[54] Rather unusually in the chemistry of plastic scintillators, this copolymer is not

obtained as bulk material, but is previously prepared from the reaction of styrene and maleic anhydride in a mixture of toluene and diethyl ether (90:10), initiated with AIBN at 60°C. ^{6}LiOH is then added to give the deprotonated polymer; but the Authors assumed that lithium was ultimately transferred from the matrix to the salicylic acid fluorophore. The overall mixture was cast on acrylic disks to afford 200 µm thin films. Despite a visually transparent sample, reported transmission is rather low with a 78 % average value between 360 and 600 nm. The maximum ^{6}Li loading obtained that resulted in a transparent film was 4.36 wt%. The Authors report an average light yield of 360 photons per thermal neutron capture event in the presence of a shielded ^{252}Cf source.

It is noteworthy that other publications cited hereafter in this Review include Lithium loading but are classified upon other criteria.

2.6.3. Heavy metal loading

Another important interest in metal loading in a plastic matrix is to make denser it and to increase its effective Z (Z_{eff}). But heavy atoms tend to have a strong fluorescence quenching due to multiple vibrational relaxations. Nevertheless a compromise can be found between higher absorption and lower light output. A polystyrene-based scintillator was successfully prepared with 17 wt% of tetraphenyltin (5.5 wt% of Sn, Scheme 8a). [55] This loading diminished the light output by 30 % (≈ 7,000 ph/MeV) compared to an unloaded scintillator; it was also noted that mechanical properties were lowered. The lack of popularity of Tin loading can also be explained by the high toxicity of organo-tin compounds. Organo-lead compounds are also hazardous but the possibility to have an important Z_{eff} motivated further study. Tetraphenyl lead (Scheme 8b) was a first candidate with very similar result as for tetraphenyltin.[55]

We just saw that methacrylic acid is a good medium to incorporate Li atom in the matrix, but methacrylic acid was previously used as a Lead chelating agent, thus allowing loading a larger amount of lead in a polystyrene matrix (Scheme 8c). [56] Lead accounts for up to 22 wt% of the

total mass giving the densest plastic scintillator ever published: 1.55 g/cm^3. First generation lead to modest scintillating materials (≈ 1,000 ph/MeV), but major improvement was performed recently with bismuth-loaded, red scintillating plastic scintillators, leading to > 5,000 ph/MeV.[57] Application has already been found for this plastic as there are uses in the Laser Mégajoule facility in Bordeaux, France, to be implemented in a hardened x-rays imaging system in a high radiative background (Figure 14).[58]

As a complementary note, PMMA can be chemically transformed to blend in inorganic compound. A major application is to create transparent x-ray or neutron shield,[59] but this will not be developed in this review.

Bismuth is also very attractive as it is the heaviest nonradioactive element and its organo derivatives are less noxious. Triphenylbismuth (Scheme 8d) is fairly soluble in styrene and allows reaching high incorporation percentage. Recently Cherepy and Payne published a series of studies[60] on such a polymer with a 40 wt% loading of $BiPh_3$ (19 wt% of Bi atom) in a PVK matrix. They evaluated the response of two different secondary fluorophores (PVK should be considered as a primary fluorophore): DPA (9,10-diphenylanthracene) and *fac*-Irpic (fac iridium-bis-(2-phenylpyridine)-picolinate). They distinctively observed a photoelectric peak and the escaping x-ray peak on the pulse height spectra with ^{137}Cs, ^{22}Na or ^{57}Co gamma sources (Figure 15). Beyond the scope of this review as the goal is not devoted to plastic scintillators, another team has focused on a different method to include bismuth in plastic scintillator: linking it to a monomer and then polymerizing it (Scheme 9).[61] Only Bi(III) complexes are used and most generaly their phenyl or bulky alkoxy derivatives due to their relative stability and their low absorption in the visible spectrum. But it is still very difficult to obtain a clear plastic scintillator as radical conditions tend to degradate Bi complexes and make the scintillator yellowish (absorption around 300 – 400 nm).

In order to understand the intrinsic influence of bismuth doping and heavy atom fluorescence quenching, a systematic study on various Bismuth complexes was performed by Hamel *et al*.

Bismuth organometallics were synthesized using two main paths: Grignard chemistry (Li and Mg), and acid-base ligand exchange (Figure 16a). These complexes embedded in a PS matrix succeeded to match commercial lead loaded scintillator performances and are a target of choice to achieve low energy gamma spectrometry.[62] The Figure 16b presents the evolution of an ^{241}Am pulse area spectra versus bismuth loading, showing a clear increase of the photoelectric peak, each spectra were recorded in only 15 seconds with a 20 kBq source, demonstrating this technology readiness for field deployment. Substitution of Pb by Bi answers the concern of toxicity, which can be an industrial prospect as Bi-doped plastic scintillators are not commercially available.

The spectral and temporal characteristics of x-ray luminescence of composites consisting of microparticles (1 – 20 μm) of "heavy" components (oxides, fluorides and sulfates of Zn, Cd, Cs, Ba, La, Lu, Hf, Pb, Bi) and an organic polymer binder (typically polystyrene / PPO / POPOP) impurities have been investigated.[63] Among the composites studied, the highest light yield was achieved for the system consisting of LaF_3 with polystyrene activated with PPO + POPOP. No information was given about the morphology of the corresponding PS.

2.6.4. Fluorinated scintillator

A collaboration between Polish and French teams has led to a proof-of-concept of fast neutron/gamma discrimination using the energy threshold of the reactions n(^{19}F,^{16}N)α or n(^{19}F,^{19}O)H^+.[64] Indeed, the energetic gap allows discriminating neutrons with E > 2.5 MeV with less energetic neutrons and gamma. To reach this, PSt has been replaced by poly(2,3,4,5,6-pentafluorostyrene). A very high density was observed (1.56), even higher than Pb- or Bi-loaded plastic scintillators. Light output was estimated to be close to 3,100 ph/MeV, with a decay time of 3.0 ns, and preliminary results for n/γ discrimination of a PuBe radioactive source were somehow modest but exist (Figure 17), as due to small dimensions of the sample, energy deposition of highly energetic electron from beta decay of ^{16}N and ^{19}O is rather poor.

2.7. Cross-linked polymers

Some applications may present harsh working conditions, as for instance high temperature. It is known that glass transition temperature of polystyrene, principal component of plastic scintillators, is close to 100°C and thus prevent it from use close to this temperature. Cross-linked polymers can improve this thermal stability.

Preliminary examples were found in the Russian literature.[65] Low quantity of divinylbenzene (DVB, 0.01 – 1 %) was added in the scintillator preparation, affording cross-linked PS with relative light yield equal to commercial samples (97 – 102 % light yield of BC-404).

Other examples of cross-linked scintillators can be found in patent publications.[66] Stability up to 175°C is claimed (probably under neutral atmosphere), with plastic scintillators incorporating up to 20 % of divinylbenzene, associated with *p*-*t*-butylstyrene and usual (PBD, PPO, BBO, ***p*-terphenyl** and PPBBO, α-NPO, **POPOP**, preferred compounds in bold font) or unusual (*p*-vinylbiphenyl) fluorophores. < 1 % of DVB is also used for Gd-loaded plastic scintillators.[16a]

CEA has extensively studied cross-linking for phoswich applications. A phoswich (*i.e.* "phosphor sandwich") is a combination of two scintillators showing different responses upon irradiation, usually a fast and a slow decay time scintillators. More specifically, the challenge was to combine two cross-linked plastic scintillators without the use of optical cement or glue, for beta/gamma discrimination.[67] Thus, the ΔE/E discrimination gives the access to the full energy of the β^-. So, a 150 – 700 µm thin, 3 ns fast plastic scintillator was coupled to a 1 mm thick, 80 ns slow plastic scintillator, all of them displaying scintillation wavelengths centered at 420 nm (Figure 18). This technology has been successfully applied to the proof of concept of a whole contamination meter (Figure 19).

2.8. Side chain modification

Besides using the carboxylic group to incorporate inorganic elements, simple chemistry can be performed to link organic dyes to the monomer. It enables the design of polymer with more

or less proximity between dyes. In some cases such as stilbene or 1,8-naphthalimide, delay fluorescence due to a bi-molecular interaction can be observed. It has been proved that neutrons are more prompt to give rise to more localized energy deposit than gamma radiation, so this delayed bimolecular fluorescence can be used to discriminate between neutron/gamma ionizations. Delayed fluorescence gives a longer pulse and can be separated *via* pulse shape discrimination (PSD). Hamel *et al.* did the first attempt of this, with the synthesis of 1,8-naphthalimide dye (Scheme 10a) linked to different polymer chains,[68] including PMMA derivatives. Unfortunately PSD was not significant. The same approach was performed with the synthesis of stilbene substituted polymer[69] (Scheme 10b), which is single component plastic scintillator, but result did not show clear response. Side chain modification can also be a tool for more fundamental experiment. A study by Adadurov *et al.* shows that partial substitution of the methyl with a benzyl group (*i. e.* benzyl methacrylate) can be used to probe the formation of excimer and their impact on the scintillation yield.[70] We can also note that MMA substituted with fluorescent probe were used to monitor the polymerization rate under ionizing condition,[71] but this is outside the scope of this paper.

Finally, it was already mentioned the patent from Simonetti *et al.* concerning the use of *p-t*-butylstyrene instead of former styrene for polymerization of plastic scintillators.[66]

2.9. Sol-gels

Although sol-gel materials can be considered as inorganic structures, one has to admit that they are prepared from organic molecules. Since the 2000's, identical developments have been performed, mainly by the collaboration of Dai and Wallace's groups. They all include loading sol-gel materials with thermal neutrons-sensitive elements, such as Lithium, Gadolinium or Boron.

Table 3 references the main characteristics of each scintillator. Both Boron- or Lithium-enriched sol-gel scintillators were produced in 109. Gel containing enriched $^{10}B(OH)_3$ was not discernibly sensitive to thermal neutrons (originated from thermalized AmBe of ^{252}Cf sources)

at all, contrary to Lithium-loaded materials. All these scintillators were also tested under alpha irradiation.

The Europium-doped gadolinium oxide sol-gel was irradiated with 14 keV x-rays. Imaging of a 30 µm thick tungsten wire was possible (Figure 20).[110]

The work performed by Kesanli *et al.* deals with the preparation of a hybrid polystyrene-silica nanocomposites in the presence of arene-containing alkoxide precursor through room temperature sol-gel processing, affording transparent monoliths.[111] Lithium-6 salicylate was used as the neutron sensitizer, with different ^{6}Li-loadings, ranging from 0.5 to 1.0 wt%. The key-molecule is 3-(trimethoxysilyl)propyl polystyrene, which allows efficient scintillation energy transfer while being integrated inside the sol-gel matrix. Surprisingly the fluorophores were added as a liquid scintillation cocktail. Neutron detection results are discussed in terms of pulse height spectra, relative to commercial neutron-sensitive inorganic scintillator KG2.

In their following publication, various fluorescent compositions were tested (two organic and seven inorganic), following the same lithium loadings (1.5 wt%).[112] The light emission spectra of the scintillators and their pulse shapes were measured, but no clear statement was done as which composite scintillator would be the best.

Boron-loading was performed by Koshimizu *et al.* Boron was directly linked to the main chain *via* the condensation of trimethylborate $B(OMe)_3$. The scintillation characteristics were examined under He irradiation, and it was found that the scintillation intensity increased with the concentration of poly(ethylene glycol) PEG. It also increased linearly with the concentration of butyl-PBD. The Authors specified that approximately half of the prepared samples could be successfully fabricated into monoliths without cracking.

A second use of luminescent europium cation in sol-gels has been described in the literature, for the detection of γ rays.[114] The behavior of the luminescence spectra of the excited states of rare earth indicates a strong, linear dependence with gamma radiation doses, up to 400 Gy. Similar results were also obtained for Tb-doped silica gel. Another modification of the

fluorescent probe includes a 2,5-diphenyloxazole-derived molecule, covalently linked to the sol-gel macrostructure *via* either a hydroxymethyl or a urethane linkage at the 4-position.[72] Results were confronted with standard PPO entrapped in the sol-gel matrix. First the PPO derivatives were compared by liquid scintillation counting, and then they were compared altogether by detecting low energy β^- radiation emitted by tritium. Preparation of sol-gel scintillators afforded transparent, fracture-free colorless materials.

Surface-functionalized carbon quantum dots (CQDs) entrapped in sol-gel xerogels were used for the first time by Quaranta *et al.*[115] CQDs were obtained from thermal decomposition of citric acid in the presence of hot [3-(2-aminoethylamino)propyl]trimethoxysilane, giving rise to materials with decay time estimated close to 4 ns and 26 % quantum yield. These materials were not tested so far for ionizing radiation detection.

Although interesting, in particular for their high density suitable for γ spectroscopy, all these materials suffer from a lack of possibility to prepare large volumes of scintillators. They are therefore limited to the detection of particles with low linear energy transfer.

2.10. Miscellaneous

2.10.1. Extrusion and molding

Whereas probably 99 % of the production of plastic scintillators is performed by bulk, thermally initiated polymerization, the group of Pla-Dalmau has studied the potential of extruded PS, as for optical fibres (Figure 21).[42,73] Starting from PSt or PVT pellets or powders, an extension of this work includes loading with inorganic powders such as Lithium or Boron for thermal neutron detection.[42] Quality of materials and fluorophores, as well as the conditions for extrusion (air *vs*. neutral atmosphere) is discussed. They claim a production cost 5 – 9 times cheaper compared with cast scintillators, albeit with slightly reduced optical properties.

Almost in the same time, the Institute of High Energy Physics in Russia reported molded and extruded PS.[65,74] Melting was performed around 200°C and the melt was extruded through a spinneret. Extrusion was realized with various organic dyes and (in)organic fillers. The Authors even tried combination of two polymers, e. g. polystyrene with polyethylene, polyisobutylene or polypropylene, giving rise to scintillators with low levels of optical transmission.

Application of such extruded PS has been recently reported for measuring antiproton annihilations.[75]

2.10.2. Quantum dots (QD)

Quantum dots (QD) offer numerous advantages such as tunable emission wavelength, fast response time, thermal and chemical stability and thus could be used as fluorophore for radiation detection. Nevertheless, the incorporation of quantum dots in a polymer matrix is challenging, as the QD aggregation must be avoided in order to prevent luminescence self-quenching. Several strategies such as chemical modification of the QD's surface or incorporation in a prepolymer have been developed. Tomczak *et al.* have published a review[76] dealing with the design of QD-polymer hybrid material and this aspect will not be discussed herein.

The first example involving the utilization of quantum dots for radiation detection was published by Létant and Wang in 2006.[77] Nanoporous glass was impregnated with CdSe-ZnS QD solution. The obtained QD-glass hybrid material offers an excellent energy resolution (2 % at 59 keV) compared with standard inorganic NaI(Tl) (6 – 7 % at 662 keV) but the acquisition time required is very long due to the low amount of photons emitted by the system. Rhodamine B-based scintillator shows a scintillation output significantly higher than its QD counterpart. These results have been attributed by the authors to the larger Stokes shift of rhodamine compared to cadmium QD. Quantum dots usually suffer from small Stokes shift (20 to 40 nm) leading to photon reabsorption and contributing to lower the quantum

efficiency of the scintillators. Rogers *et al.*[78] described the preparation of transparent PMMA scintillators loaded with 0.5 wt% CdTe quantum dots. The authors evaluated different quantum dots sizes, emitting from 520 to 600 nm and different polymer volumes, geometries and thicknesses but only observed very low count rates (8 to 10 counts per minute with an ^{241}Am source). They also attributed this lack of efficiency to small Stokes shift of the quantum dots and the small quantum efficiency of the photomultiplier at the QD emission wavelength.

In order to prevent self-absorption, quantum dots can be used not as emitters but as antenna. Campbell and Crone[79] have published the first example of radiation detection using QD in a polymer matrix. CdSe/ZnSe QD are surface-passivated with hexadecylamine and incorporated in the semiconductor polymer poly[2-methoxy-5-(2-ethylhexyloxy)-1,4-phenylene-vinylene] (MEH-PPV). The polymer was dissolved in chloroform with QD volume fraction from 0 to 21 % and was spin casted on sapphire substrate. The absorption and photoluminescence (PL) spectrum (Figure 22a) of the polymer are slightly affected by the QD incorporation in polymer matrix. Quantum dots have higher ionization energy than the polymer; radiations thus mainly produce excitation of the inorganic QD that subsequently transfer their energy to the organic polymer matrix *via* Förster energy transfer.

The cathodoluminescence (CL) was measured using 3 keV electrons at a current of 30 pA and normalized to the pure MEH-PPV emission (Figure 22b). The CL increased linearly with the QD concentration for volume fraction between 0 and 15 % but it dramatically decreased for the 21 % QD doped film. Optimum CL intensity was expected by the authors for a QD volume fraction of 40 %, but the phase separation was observed by scanning electron microscopy (SEM) for a QD volume fraction higher than 15 %, responsible for the cathodoluminescence decrease. Polymers doped with a primary fluorophore have been investigated in order to enhance the light output of QD-based plastic scintillators.[80] Optimal

radioluminescence intensity was found for a polystyrene matrix loaded with 0.4 wt% of PPO and 0.1 wt% of CdSe quantum dots.

QD are good candidates for the enhancement of the spatial resolution of x-ray detection. Water soluble CdTe quantum dots[81] capped with mercaptopropionic acid (MPA) were dispersed in polyvinyl alcohol (PVA) and thin films were spin-coated on glass substrate. It was possible to obtain a transparent 30 µm film with 2 wt% of QD. Transparency decreased when the thickness of the film or the amount of QD increased due to segregation of the quantum dots. Transparent bulk sample of PMMA doped with 0.5 wt% QD showing a thickness between 10 and 20 mm were prepared. Hybrid PMMA/QD polymers were tested for x-ray detection (Figure 23), and showed better spatial resolution (5 lines/mm) than the commercial Gd_2O_2S/Tb screen (2.8 lines/mm).

The possibility to load polystyrene/CdSe scintillators with the commonly used PPO was studied by Lawrence *et al.*[82] The Authors have described the preparation of polystyrene loaded with PPO and/or QS (Table 5).

Under x-ray radiation, no significant enhancement of the scintillation was observed when the polystyrene was doped with PPO or quantum dots. However, the scintillation intensity was four times higher when both PPO and QD were included in the polymer matrix. The same trend was observed by the Authors for ^{241}Am alpha induced scintillation.

2.10.3. Composite scintillators

It is well-known that single crystals of aromatic molecules are particularly efficient scintillators. However, their high price and the difficulty to prepare big-size detectors limit their use. In this context, a strategy based on grinding single crystals and incorporating them into an inert matrix (usually Sylgard) has been developed by the Institute for Scintillation Materials in Ukraine.[83] So-called composite scintillators, made from *p*-terphenyl or stilbene have been successfully tested for fast neutron/gamma discrimination (Figure 24).[84] These composite scintillators are usually compared with their parent materials, single crystals

scintillators, in terms of decay time, light output and other performances. Large-area, stilbene composite scintillators have recently been reached (Ø 200 mm × h 20 mm),[83h] but diffusion issues seem to limit the scintillation properties of these materials while being prepared with important thickness. A dual fast neutron/thermal neutron detector based on a phoswich-based strategy with a combine stilbene composite layer and a Cerium-doped Gadolinium silicate (Ce:GSO) composite layers has also been reported by the same institute.[85]

2.10.4. Structured scintillators

Radiation Monitoring Devices has introduced the possibility to create plastic scintillators embedded in a fiber optic array.[86] Already known for filling fibers with liquid scintillators, the challenge herein proposed is to be able to polymerize liquid monomers inside the capillary with preserving optical transmission. Thus, a 36 cm² parallelepiped made from Ø 100 µm capillaries is sunk into the monomer and polymerization is processed directly into the capillaries (Figure 25). Some recipes include loading with *o*-carborane for thermal neutron detection.[86c] Good light yields were observed for PSt / PPO / POPOP / *o*-carborane, in the range 7,000 – 11,000 ph/MeV. Very good resolution was observed when the scintillator was illuminated by neutrons.

Almost in the same time, this technology has also been developed at the French Atomic Energy Commission for the fibering of loaded plastic scintillators.[56a,87] The same technology to potentially image x-ray sources has been applied to Laser Mégajoule facility.

2.10.5. Microspheres and Polymer dots

Commercial PS microspheres are available from Saint-Gobain or Detec-Rad but they can also be prepared by evaporation/extraction process. Typically an organic phase containing the polymer and the dyes is slowly added to a vigorously stirred aqueous solution. The organic phase in slowly evaporated and the polymer spheres are then filtered. Depending on the polymer concentration, spheres from few nanometers (polymer dots) to micrometer

(microspheres) scale can be prepared. Such polymers appear to be an alternative to liquid scintillation for the quantification of alpha and beta emitters because it does not generate mixed wastes after the measurement.[88]

Scintillation properties of microspheres prepared from PSt doped with various, classical fluorophores: *p*-terphenyl, PPO, POPOP, bis-MSB and naphthalene, with a typical diameter of *ca.* 130 µm were investigated. Detection efficiency values obtained with these synthesized microspheres for ^{3}H, ^{14}C, $^{90}Sr/^{90}Y$ and ^{241}Am sources are better than those obtained using commercial plastic scintillation microspheres.

Osakada *et al.* prepared water-soluble polymer dots (26 - 35 nm diameter) doped with an iridium complex in order to achieve x-ray computed tomography.[89] Poly(vinylcarbazole) mixed polystyrene graft ethylene oxide functionalized with carboxylic end group (to enhance the water-solubility of the polymer dots) with an iridium complex dye were prepared as described above. Under x-ray radiation, the iridium polymer dots dissolved in water are five time more luminescent than iridium complex in THF or non-doped polymer dots in water solution.

2.10.6. Poly(ether sulfone)

The same group who extensively studied PEN and PET polyesters recently reported the first example of poly(ether sulfone) as scintillation material.[90] Again, the polymer scintillates by itself. An extremely high refractive index of 1.74 and a 1.37 density are shown (1.58 and 1.04 for PSt, respectively). Scintillation yield was in the range 3,000 – 5,000 ph/MeV. Despite its amber color, the material is able to fluoresce at 350 nm. Contrary to PET and PEN, a significant size of scintillator has been prepared, with dimensions 31 × 31 × 5 mm^3 (Figure 26). This material was confronted to alpha radionuclides such as ^{241}Am and ^{252}Cf.

3. Modification of the fluorescent probe

3.1. Organometallic complexes

Ionization of a polymer matrix statistically leads to the formation of 25 % of singlet excitons and 75 % of triplet excitons.[91] Only the singlet excitons are collected in standard organic scintillators. Organometallic phosphorescent complexes are very promising chromophores for scintillation applications. The heavy atom induced spin-orbit coupling allows them to radiatively emit from both singlet and triplet states. The utilization of iridium complexes in OLEDs already allows the preparation of system with quantum efficiencies close to 100 %. Campbell and Crone[92] published examples of 5 µm drop-casted PVT and PVK films doped with iridium(III) tris(2-(*p*-totyl)pyridinato) (so-called $Ir(mppy)_3$) complex. The amount of iridium complex in the films varied from 1 to 35 wt% in PVT and from 0.04 to 10 % in PVK. The scintillation response of these films as a function of wavelength (Figure 27a) were obtained *via* excitation of the samples with a 10 keV electron gun.

A mono-exponential decay of approximately 850 ns is observed for both matrices. The spectrally integrated scintillations yield were measured using EJ-232 (8,400 ph/MeV) PS as a reference. Figure 27b shows the estimated scintillation yield as a function of $Ir(mppy)_3$ wt% in plastic, the scintillation yield is enhanced as the amount of complex increases in the plastic. The Authors claim a scintillation yield of 30,000 ph/MeV for an $Ir(mppy)_3$ content of 20 % in PVT and 4 % in PVK. The scintillation is assumed to be more efficient in PVK matrix due to a better energy matching between the polymer and the organometallic fluorophore. Rupert *et al.*[60] described a system composed of a PVK matrix incorporating an iridium complex (FIrpic) or 9,10-diphenylanthracene (DPA) and doped with high-Z triphenyl bismuth ($BiPh_3$). Most of the Bismuth-loaded scintillators are made of PVT, incorporation of a high amount of heavy atoms mainly leads to a decrease of the scintillators light yield, PVK has a low excited state energy and its use prevents quenching of the light yield induced by $BiPh_3$. When the amount of $BiPh_3$ increases from 0 to 40 % the beta radioluminescence decreases for DPA-based

scintillators and slightly increases for the FIrpic-containing scintillators. This behavior can be explained by an augmentation of the triplet population induced by the bismuth.

Gamma-ray spectra were acquired with ^{137}Cs and ^{241}Am, were fit with a spectrum simulator and scintillation yield were determined by comparison with EJ-208 Compton edge (Table 6). The best scintillation yield was achieved by the 3 % FIrpic / 40 % $BiPh_3$ scintillator; however the results are still lower than commercial EJ-208. A better energy resolution and 25 fold increase of the photoelectric peak height is observed for the bismuth-loaded samples.

Another advantage of organometallic-based PS is that they can achieve detection of fast neutrons and gamma rays by pulse shape discrimination. Signal for gamma ray can be attributed to the fluorescence of the plastic scintillators (arising for the singlet state of the fluorophore) and fast neutron response is peculiar to delayed emission caused by triplet-triplet annihilation. An example of PSD achieved with an iridium complex in a polymeric matrix was described by Feng *et al.*[93] The authors prepared a PVT polymer doped with the 0.1 – 0.2 wt% iridium complex $Ir(ppy\text{-}F_2)_2(F_2\text{-}pic)$. When ionized by an AmBe source, the scintillator shows a bi-exponential decay with a prompt and a delayed signal (respectively assigned to the fast neutrons and gamma response). In order to access the PSD efficiency of the iridium doped scintillator, PSD Figure Of Merit (FOM, the separation between the neutron and the gamma events divided by the sum of the FWHM values for the distributions) where performed. The PVT/Ir scintillators has a PSD capability (FOM = 1.4) lower than the commercial liquid scintillator EJ-301 (FOM = 2.1). The scintillator also has a low gamma rejection ratio, at trigger level set to an energy threshold of 400 keVee, 98 % of the fast neutrons are detected. Using EJ-204 as reference (10,000 ph/MeV), the light yield of this system was estimated at 7,400 ph/MeV. Polyvinylcarbazole (PVK) was doped with 0.025 to 0.2 wt% of $Ir(ppy)_2(acac)$. Cathodoluminescence of the different samples (Figure 28a) shows an augmentation of the iridium-centered luminescence at 515 nm and only a small decrease of the PVK emission at 420 nm when the iridium concentration is increased.

In the same paper, the authors propose an unseen feature: spectral shape discrimination (SSD). Samples were irradiated with 20 keV electron beam to simulate the scattered electron generated gamma ionization and with 2 MeV proton beam to simulate the recoil proton generated by fast neutron ionization (Figure 28b). In the case of gamma ionization, both luminescence of the matrix host (PVK) and the guest (iridium complexes) can be observed, whereas in the case of fast neutron ionization, only the iridium-centered luminescence is observed.

On the same basis, the group of Adadurov reported twice the use of two different fluorophores in PS, one for collecting singlet states (1,4-dimethyl-9,10-diphenylanthracene, with addition of the wavelength shifter 1-phenyl-5-(4-methoxyphenyl)-3-(1,8-naphthoylen-10,20-benzimidazole-4)-2-pyrazoline) and Eu(phen)$(DBM)_3$ for triplet states.[94] So herein TTA are not used for n/γ discrimination, but the large decay time difference between the two dyes is exploited. The properties are described in the Table 7.

Hamel *et al.*[95] incorporated iridium complexes in polystyrene-based cross-linked copolymer instead of the poly(vinylcarbazole) matrix commonly used in the examples cited above. Samples with 29 different iridium complexes were thus prepared (Scheme 12). Theses samples exhibited modest scintillation yields (in the range 400 - 1,500 ph/MeV) due to the low loading of iridium complexes within the matrix (0.02 - 0.05 wt%) and an unoptimized Forster Energy Transfer. Higher amounts of complexes did not improve scintillation yields, this behavior could be explained by the low solubility of most of the organometallic complexes in the monomers and high absorption of the samples when increasing organometallic concentration. Scintillators doped with $Ir(piq)_2(acac)$ showed unexpected thermoluminescence (Figure 29).

Whereas most of the work is focused on the incorporation of iridium complex in a polymer matrix, Adadurov *et al.* published a study on the preparation of europium complex-based scintillators.[96] Thin polystyrene films (50 to 150 µm) loaded with the europium complex

$Eu(DBM)_3(phen)$ in the range 0.5 to 4 wt% were prepared (Scheme 11). Under alpha radiation, the scintillation yield increases with the europium concentration of the complex reaching a maximum of 5,650 ph/MeV for the 4 wt% film. Scintillation yield of film incorporating other europium complexes[96b] ($Eu(DzA)_3(phen)$, $Eu(BPA)_3(phen)$ and $Eu(acac)_3(phen)$) showed lower values (respectively 91, 85 and 2 % of $Eu(DBM)_3(phen)$ emission intensity).

Unfortunately the utilization of these complexes in plastic scintillators requires long integration time (≈ 0.25 s) because europium have very long emission lifetime (≈ 500 µs) compared to classical organic fluorophores (few nanoseconds).

Europium and terbium complexes were also claimed as efficient fluorescent probes for scintillation in a patent.[97] The global structure of Eu(III) complexes is made from di-ketones and phosphine oxide. These compounds, embedded in a polymer matrix such as polystyrene of polysiloxane seemed to be sensitive to tritium.

3.2. Ionic liquids

This new family of scintillators is close to the boarder since it should be more seen as a composite, fully organic scintillator. The technology provides a single molecule which is able to act as both the matrix and the fluorophore. Chemical engineering can offer materials with finely tuned properties, such as liquid/solid, glass transition, emission wavelength, light yield, etc. Thus, a collaboration of French physicists and chemists from Strasbourg claimed the use of a fluorescent molecule, usually a diphenyloxazole derivative, linked to an ionic liquid moiety (an imidazolium group).[98] Typical anions Y^- counterbalancing the imidazolium salt are Br^-, PF_6^- $C_{12}H_{25}OSO_3^-$, $C_{16}H_{33}OSO_3^-$ and $(CF_3SO_2)_2N^-$. A global structure of these materials is shown in Figure 30.

It was demonstrated that spectroscopic properties are governed by the oxazole group, with ε values in the range 60 – 95 % that of PPO, and emission spectra centered around 370 nm. Scintillation decay times are in the range 1.3 – 1.8 ns under 2 MeV protons irradiation, and

slight differences occur when the anion is changed. Used as such, this system is able to perform fast neutron/gamma discrimination when exposed to an AmBe radioactive source.

3.3. Metal Organic Frameworks

Metal organic frameworks (MOF) are crystalline periodic structures obtained by the combination of a metal ion or a cluster coordinated by a rigid polydentate organic molecule. Allendorf *et al.*[99,100] were the first team to study the radioluminescent properties of these materials. Organic scintillators carboxylate derivatives (Figure 31), such as 2,6-naphthalenedicarboxylic acid (NDC), benzene-1,3,5-trisbenzoate (BTB), 5,5'-(naphthalene-2,6-diyl)diisophthalic acid (DPNTC), 5,5'-(anthracene-9,10-diyl)diisophthalic acid (DPATC) or stilbene dicarboxylic acid (SDC) were used as organic linkers.

Cathodoluminescence (Table 4) was performed by IBIL irradiation of a single crystal and the emission intensity was compared to anthracene or *trans*-stilbene emission. CL intensity is in the same order of magnitude or even greater than the anthracene and *trans*-stilbene references (9 to 124 % of the cathodoluminescence intensity). MOFs CL emission decay can be fitted with a bi-exponential decay composed of a short component (τ_{CL}) originated from the linker fluorescence and a rather long component caused by triplet-triplet annihilation (TTA). This observation is promising as MOF materials could be able to perform pulse shape discrimination. Furthermore, MOFs are extremely radiation resistant compared to anthracene and *trans*-stilbene crystals used as reference, indeed when irradiated no new emissive species and no deformation of the crystal structure was observed. Based on this preliminary work, the authors have determined few parameters (prevent the utilization of breathing or interpenetrating MOFs, favored rigid organic linkers, etc...) that could lead to the preparation of more efficient radioluminescent Metal Organic Frameworks.

Nevertheless, this method still presents some limitations, a lot of synthetic MOFs are unstable under ambient conditions and crystals of a bigger size (few cm^3) are required for counting applications.

3.4. High Concentration

Another important breakthrough is not properly a modification of the fluorophore inside the plastic scintillator, but its addition to very high concentration. It was assumed for a long time that PS are not able to perform pulse shape discrimination (PSD) between fast neutrons and gamma. Probably based on the previous work of Brooks,[101] two groups noticed that the triplet – triplet annihilation (TTA), which is at the genesis of n/γ PSD, was not probable enough in plastics compared with liquids.[102,103] Thus, by increasing drastically the loading of primary fluorophore, the creation rate of triplets should increase and therefore their triplet – triplet interaction could occur efficiently for PSD to be achieved.

This assumption was successfully demonstrated with small, lab-scale radioactive sources such as ^{252}Cf or AmBe. A formula-derived PS from Zaitseva's recipe is currently sold by Eljen Technologies under the trade name EJ-299-33.[104] Currently, numerous research teams benchmark this scintillator under various experimental conditions.[105] But still, numerous interrogations occur since not all fluorophores, even at high concentration can perform "suitable" triplets vicinity for high TTA rates, and the commercial scintillator seems to display instability due to nucleation of PPO and morphology deformations (Figure 32).

Very recently Zaitseva *et al*. combined Lithium loading with primary fluorophore at high concentration to perform a thermal neutrons/fast neutrons/gamma discrimination.[106] This is made possible by adding to their previous PPO-loaded plastic scintillator the lithium salt of 3-phenylsalicylic acid (range 5 – 10 % to the total weight of the material, either natural or isotopically enriched to ^{6}Li, Figure 33).

As one can see, neutron/gamma discrimination is an extremely hot topic and numerous laboratories try to develop their own technology. The following Table gives an overview of the most relevant results.

CEA performed to prepare a big size plastic scintillator with dimensions > 100 mm (Figure 34). As expected, discrimination properties are lower with such size. However some

interrogations remain and the race is not over.[107] Photophysics will probably be the final tool to tune the best available PS for PSD.[102f] As an example, Blanc *et al.* were able to simulate either fast neutron or gamma interaction with a plastic scintillator by using a femtosecond LASER. Triplet-triplet annihilation was achieved when high power densities were deposited inside the matrix of the scintillator. Experiments conducted on liquid sample BC-501A, commercially available NE-102 and lab-produced neutron-gamma discriminating PS confirmed these results.

This example of recent developments on PS is certainly the most impressive in terms of uninteresting during almost 50 years, then a strong competition to find probably a suitable substitute of ^{3}He in neutron detection portal monitors.

4. Conclusion

It is really surprising to admit that > 90 % of commercial plastic scintillators available from the two worldwide suppliers, namely Saint-Gobain and Eljen Technologies, have been developed probably 30 – 40 years ago. This is probably why almost no developments occurred in the 80's and the 2000's are so interesting. It is noteworthy that the breakthrough initiated with EJ-299-33, neutron/gamma discriminating plastic scintillator developed at LLNL will incite global companies to fund chemists to find scintillators of the future. An easy comparison could be performed with LED and Si-based photovoltaic, which are slowly but surely substituted by OLEDs and organic-photovoltaic. It is thus obvious that new composite materials will replace standard scintillators. It is just a question of time.

Among all the examples cited in this text, emerging solutions for replacement of ^{3}He (neutrons detectors) seem a good competition between international laboratories. Gamma spectrometry is also one of the highest challenge chemists have to exceed in the next future. Many possibilities exist also for the detection *at the small scale, i.e.* for alpha and beta detections, mainly. Polyimides, sol-gel and other highly-absorbing or fragile materials can be really useful for this purpose.

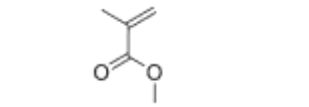

Methyl Methacrylate (MMA)

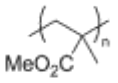

poly(methyl methacrylate) (PMMA)

Scheme 1. Monomer and general formulation of PMMA.

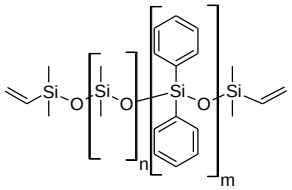

Base resin A1. m = 22-25 %

Average MW : 12500

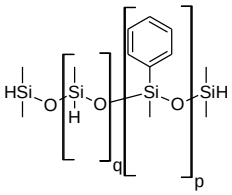

Cross linker B. p = 50 %

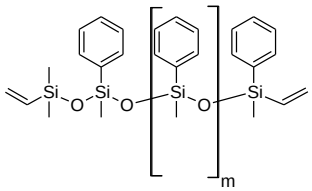

Base resin modifier A2.

Average MW : 2500

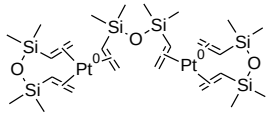

karstedt catalyst in Xylene 2.4 % Pt

Scheme 2. Standard composition of Polysiloxane rubber precursor.[17b]

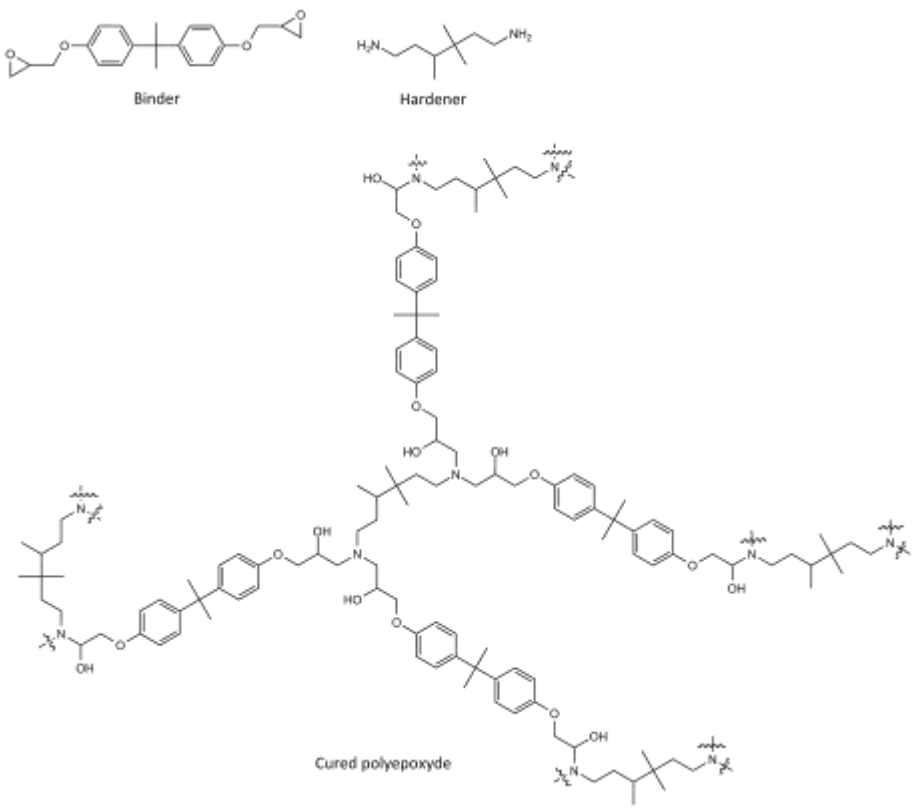

Scheme 3. An example of standard binder and hardener and their subsequent cured polyepoxyde.

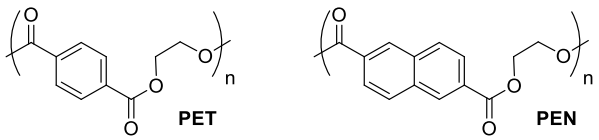

Scheme 4. Structures of poly(ethylene terephthalate) PET and poly(ethylene naphthalate) PEN.

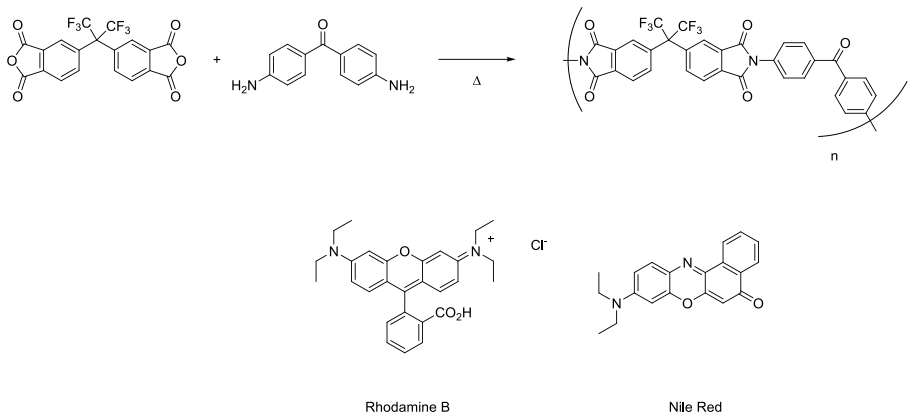

Scheme 5. Synthesis of polyimide (up) and red dyes used as dopant (bottom).

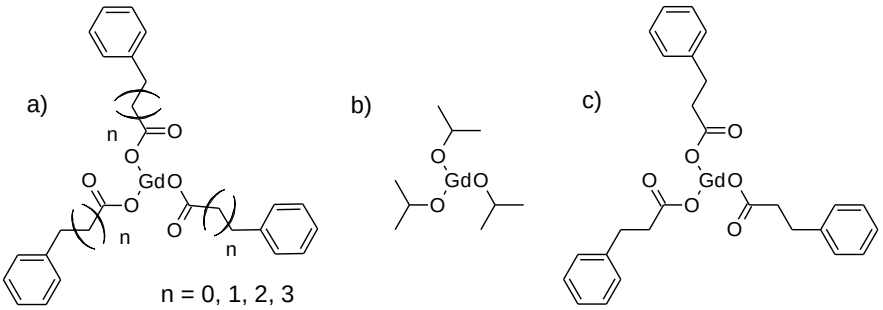

Scheme 6. Organo-gadolinium compounds soluble in classical monomers (MMA and Styrene) a) General formula of gadolinium phenyl-caboxylate;[48] b) Gadolinium isopropoxide;[46] c) Gadolinium phenyl-propionate.[50]

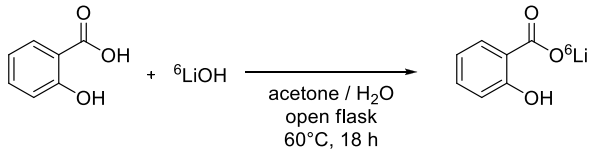

Scheme 7. Preparation of 6-lithium salicylate.

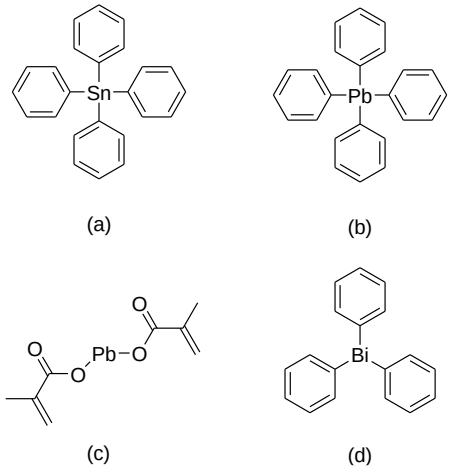

Scheme 8. Chemical formulas of various organometallic compounds (a) Tetraphenyltin (b) Tetraphenyllead (c) Lead dimethacrylate (d) triphenylbismuth.

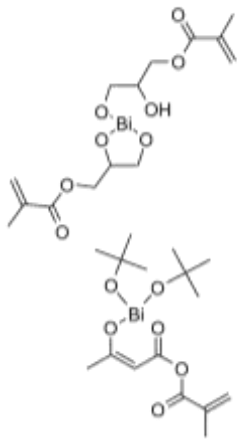

Scheme 9. Bismuth complexes linked to methacrylate moiety.[61]

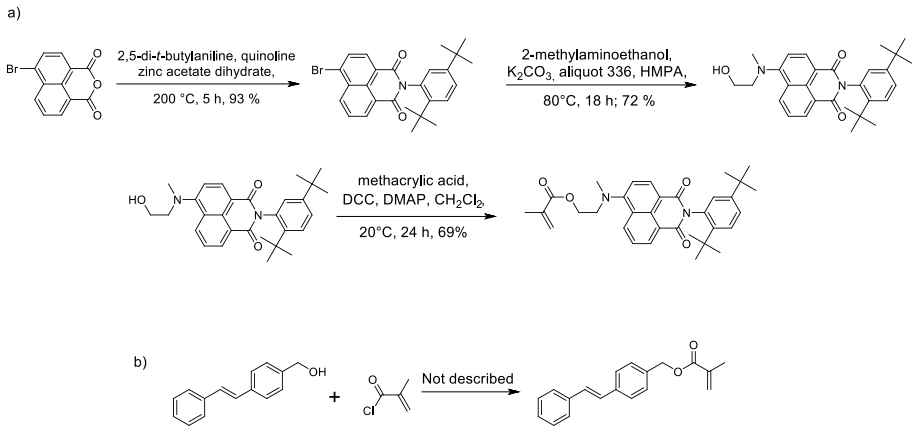

Scheme 10. Synthesis of emitters linked to methacrylic monomer: (a) 1,8-Naphthalimide dye,[68] (b) Stilbene dye.[69]

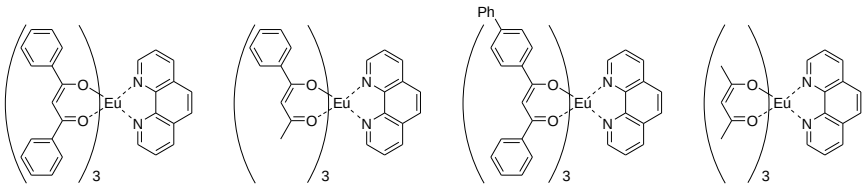

Scheme 11. Europium complexes studied.

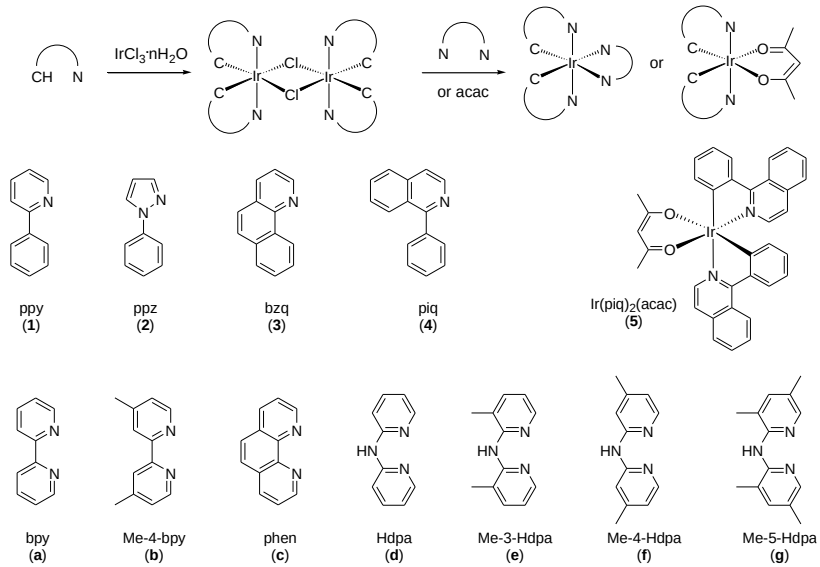

Scheme 12. Synthetic procedure and ligand used for the preparation of the iridium(III) complexes.[95]

Figure 1. Plastic scintillators displaying different emission wavelengths (excitation with UV lamp; copyright CEA).

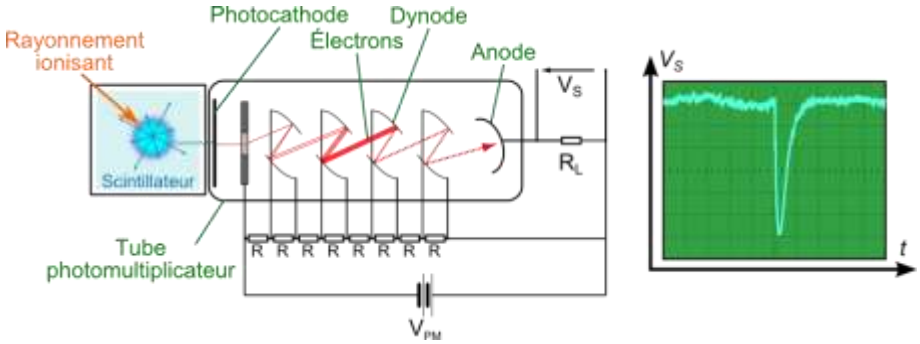

Figure 2. From ionizing radiation to electric signal.

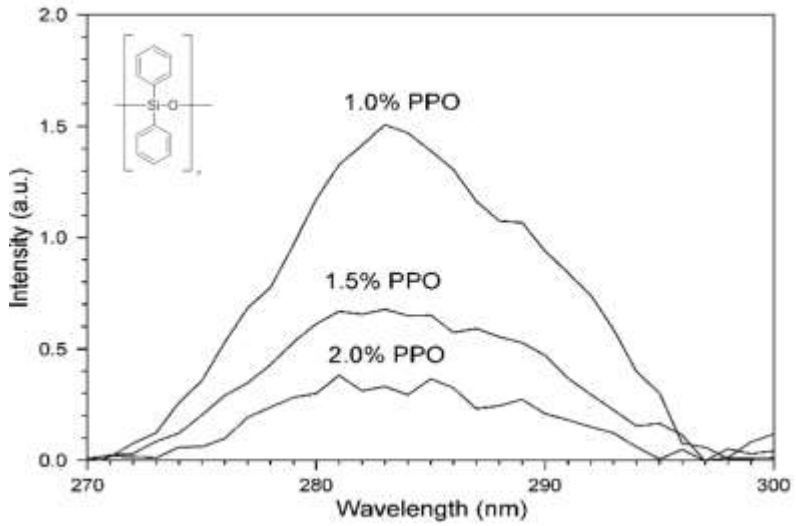

Figure 3. Emission spectra in the UV range (λ_{ex} = 250 nm) from the diphenylsiloxane unit of a standard siloxane matrix with different PPO concentrations (reproduced with permission from ref 17a. Copyright 2010 from the Authors).

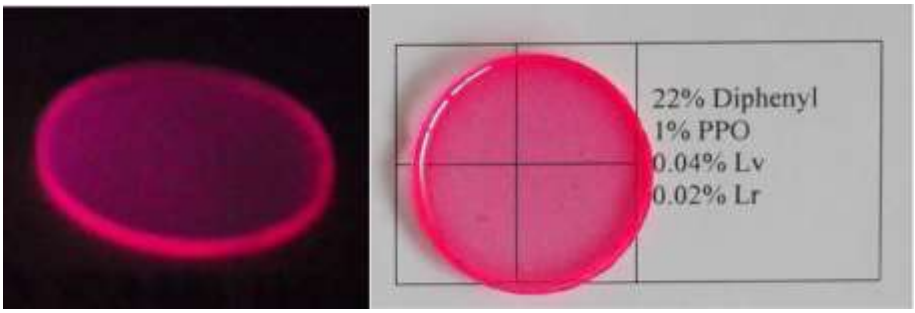

Figure 4. Polysiloxane-based red emitting scintillator irradiated by 380 nm lamp (left) and in daylight (right). Lv means Lumogen violet® and Lr Lumogen Red® (reproduced with permission from ref 17d. Copyright 2013 from the Authors).

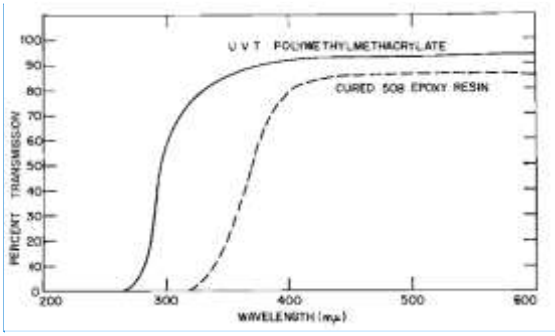

Commenté [MH2133204]:
Epaisseur des échantillons à préciser

Figure 5. Transmission percentage of a standard cured optical polyepoxyde compared to an optical PMMA (reproduced with permission from ref 23. Copyright 1968 Taylor & Francis).

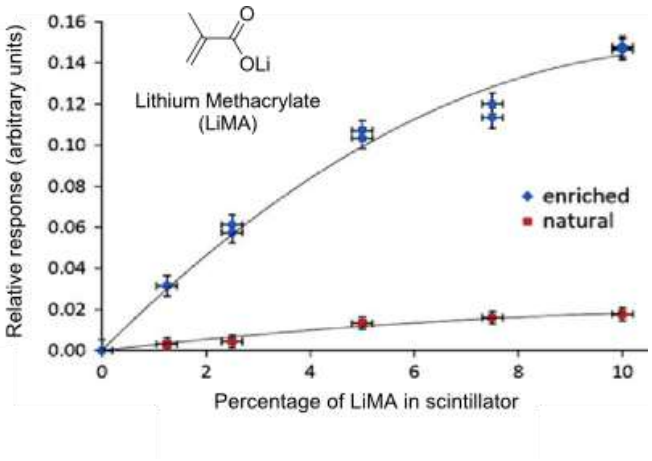

Figure 6. LiMA monomer and performance versus quantity of enriched and natural lithium methacrylate containing plastic scintillator. Measurements were conducted with a thermal neutron beam (reproduced with permission from ref 35. Copyright 2013 Elsevier B. V.).

Figure 7. Photo of scintillator samples, 1.25 wt% enriched LiMA (left) and 10 wt% enriched LiMA (right). Diameters are 20 mm, thicknesses 10 mm (reproduced with permission from ref 35. Copyright 2013 Elsevier B. V.).

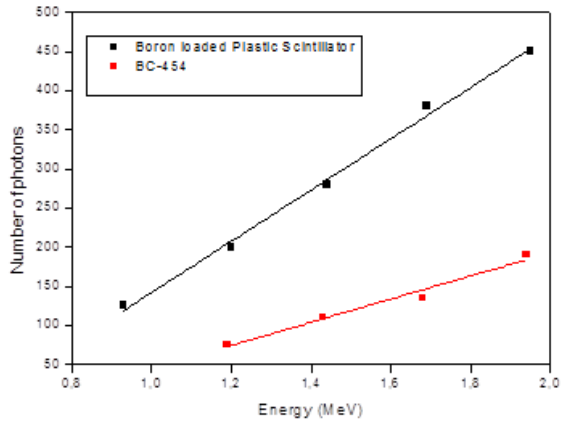

Figure 8. Comparison of Birks' fit between commercial (BC-454) and new boron loaded scintillator.[43b]

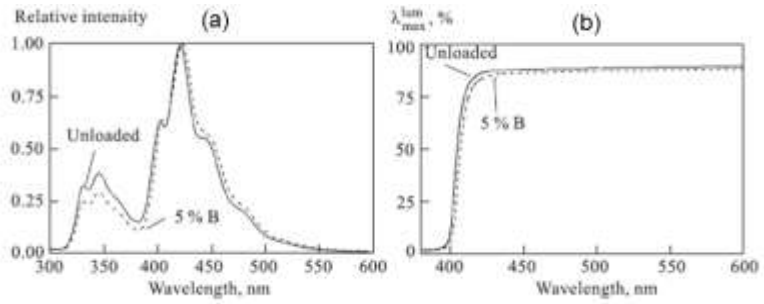

Figure 9. (a) Comparison of photoluminescence spectrum between standard and boron-doped plastic scintillator; (b) Comparison of transmission spectrum between standard and boron doped plastic scintillator (reproduced with permission from ref 44. Copyright 2001 World Scientific Publishing Company).

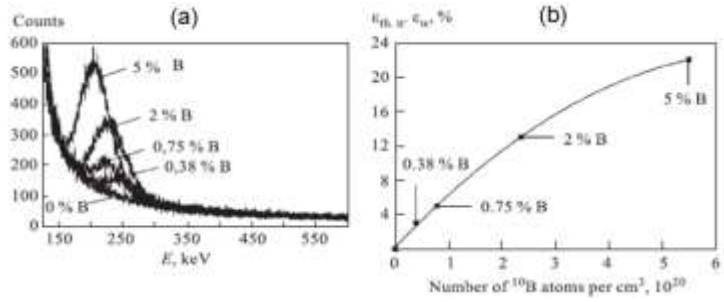

Figure 10. Evolution of neutron sensibility with boron loading (a) on a pulse height spectrum; (b) on a quantic yield versus number of ^{10}B atom by volume spectra (reproduced with permission from ref 46. Copyright 2001 World Scientific Publishing Company).

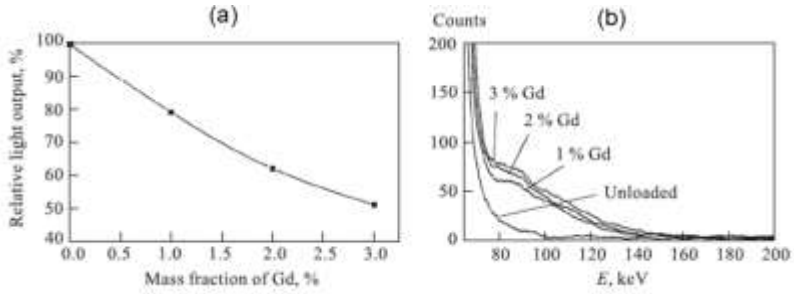

Figure 11. Evolution of neutron sensibility with Gadolinium loading (a) on a light output versus mass fraction spectra; (b) on a pulse height spectra (reproduced with permission from ref 46. Copyright 2001 World Scientific Publishing Company).

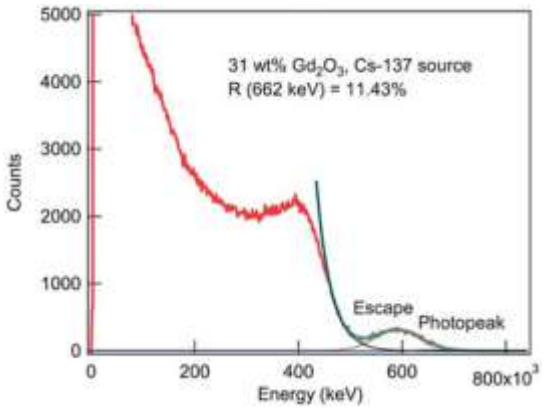

Figure 12. Pulse height spectra of ^{137}Cs with a plastic scintillator loaded with Gd_2O_3 nanoparticles. (Reproduced with permission from ref 51. Copyright 2013 Royal Society of Chemistry).

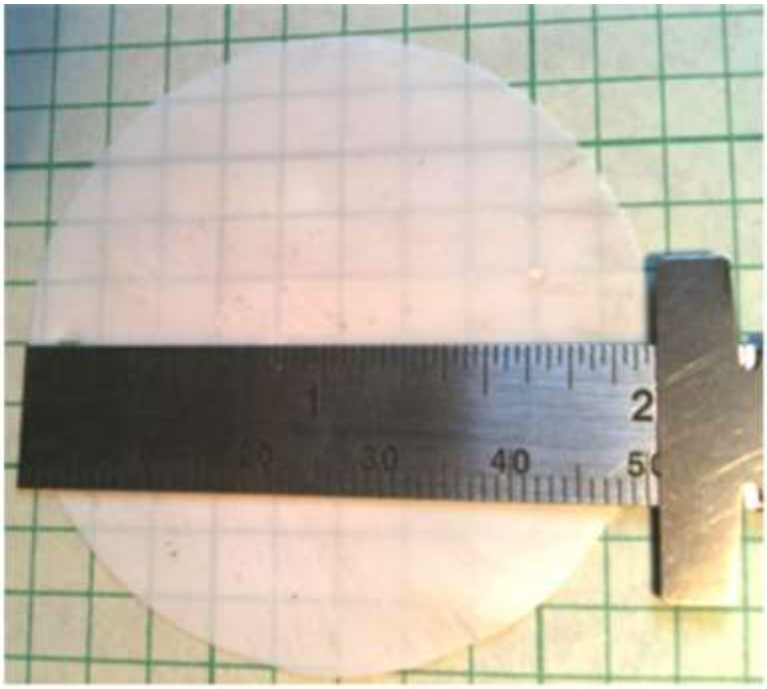

Figure 13. Example of a composite sample of thickness 110 µm and 48 mm diameter (Copyright Indraneel Sen).

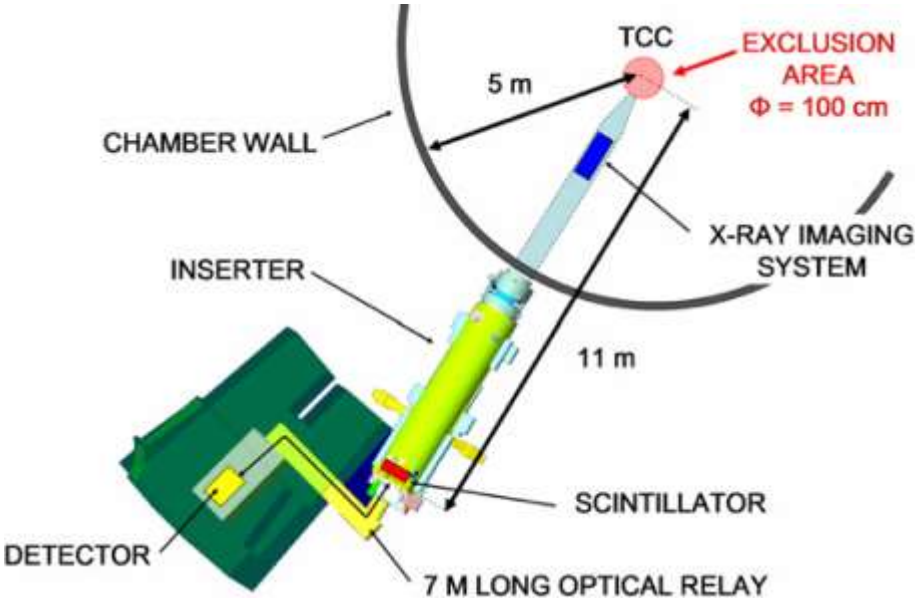

Figure 14. Diagnostic implantation in the LMJ facility.

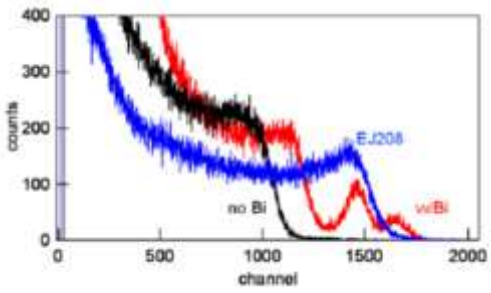

Figure 15. ^{137}Cs Pulse height spectra showing the bismuth loading influence on scintillation efficiency and the presence of photoelectric peak. (Reproduced with permission from ref 60d. Copyright 2012 Europhys. Lett.).

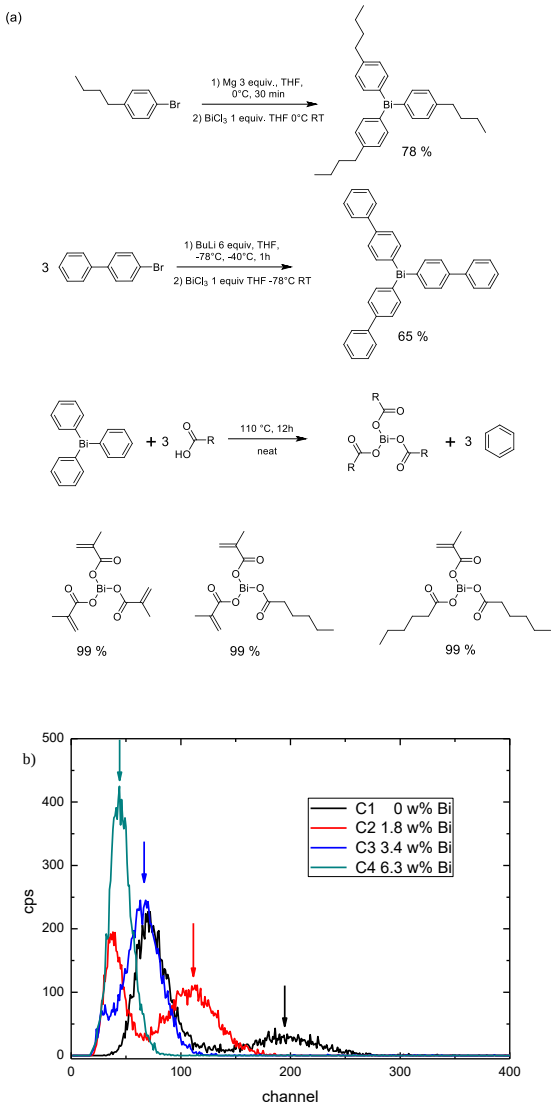

Figure 16. (a) Synthetic pathways towards organo-bismuth complexes; (b) Pulse area spectra of ^{241}Am, breaking down the loading effect on the light yield.

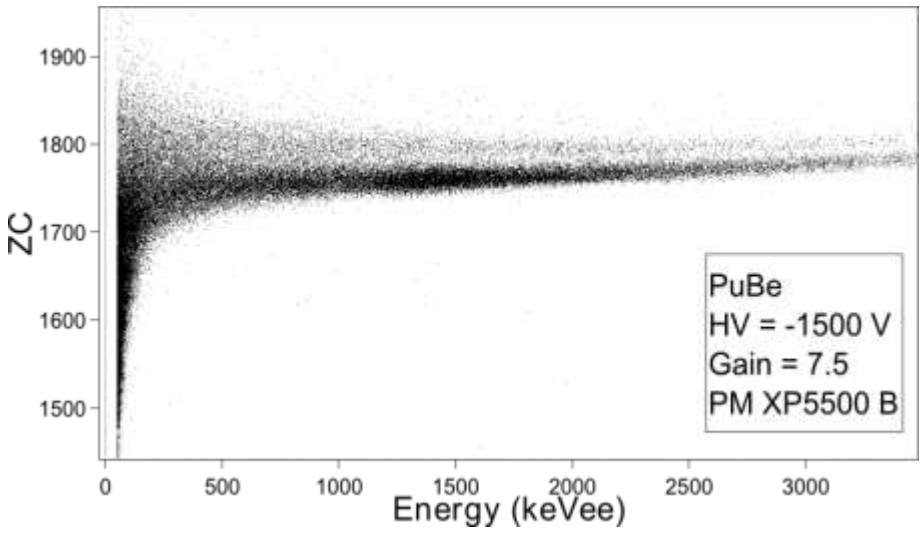

Figure 17. Neutron/gamma discrimination when irradiating the sample with a PuBe source.

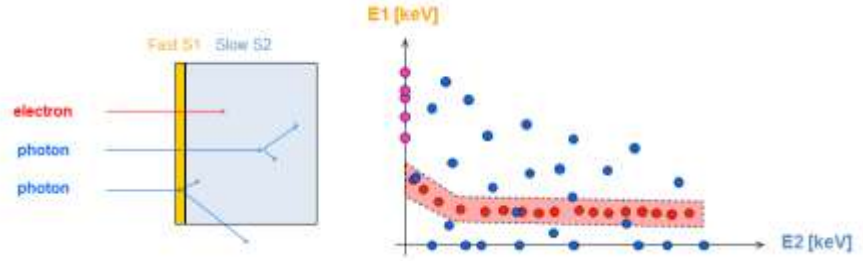

Figure 18. Principle of β/γ discrimination in phoswich scintillator. Betas appear in the pink zone in the bi-dimensional spectrum (on the right).

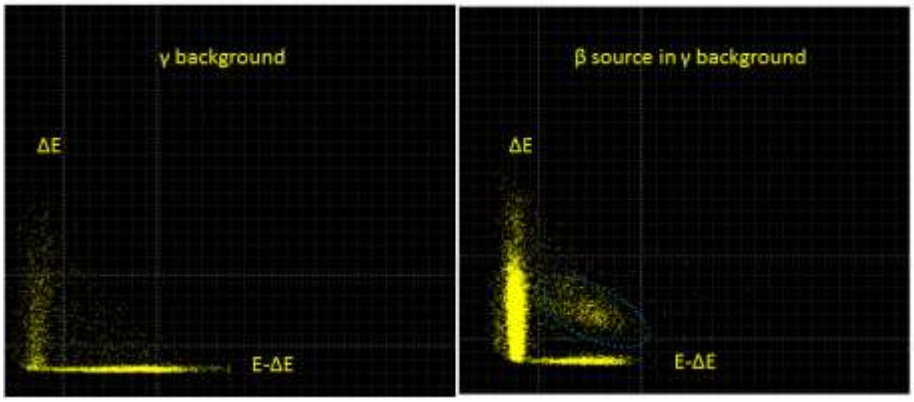

Figure 19. Results of β/γ discrimination in a phoswich scintillator with a 700 μm thin layer.

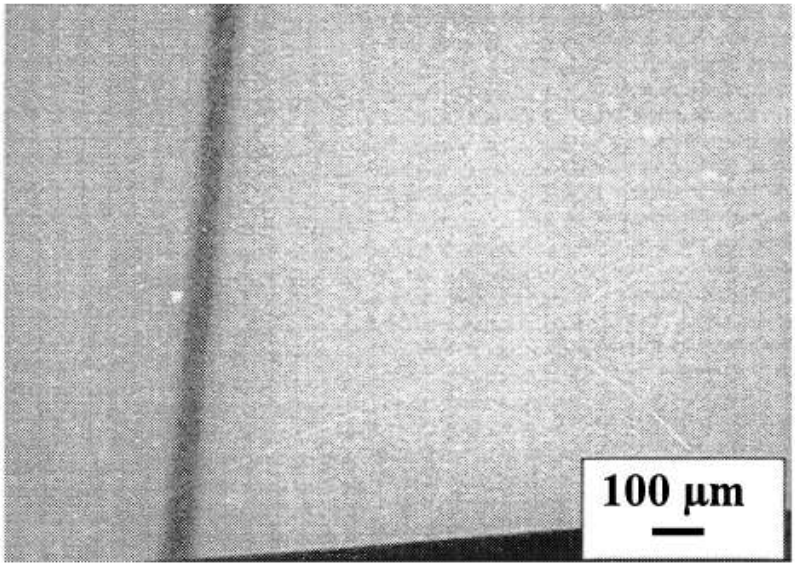

Figure 20. Eu^{3+} doped Gd_2O_3 sol gel film irradiated at 14 keV x-rays, showing a 30 μm tungsten wire (reproduced with permission from ref 110. Copyright 2004 SPIE).

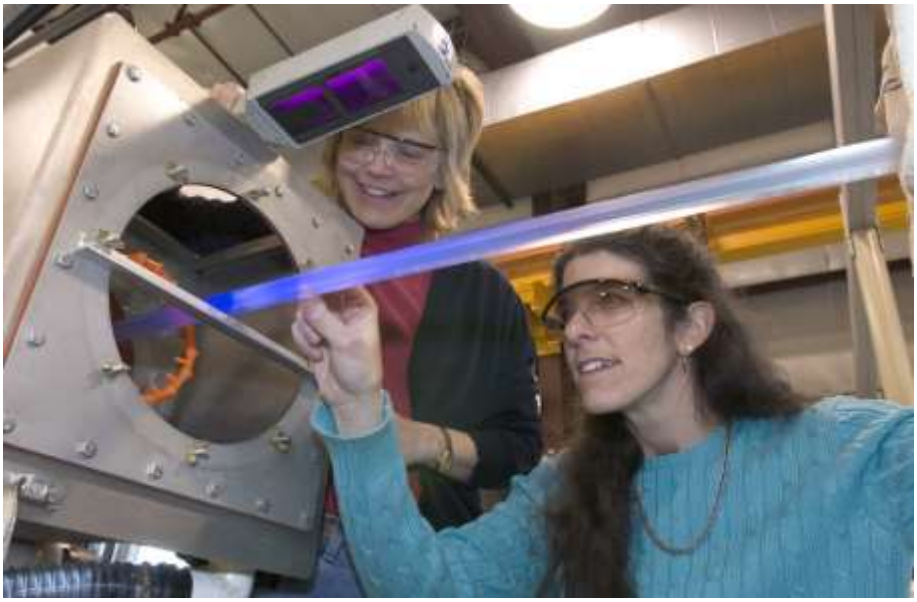

Figure 21. Extruded plastic scintillator fluorescing under UV inspection lamp at Fermilab for the MINERvA (Main INjector ExpeRiment Neutrino-A) project (Copyright United States Department of Energy).

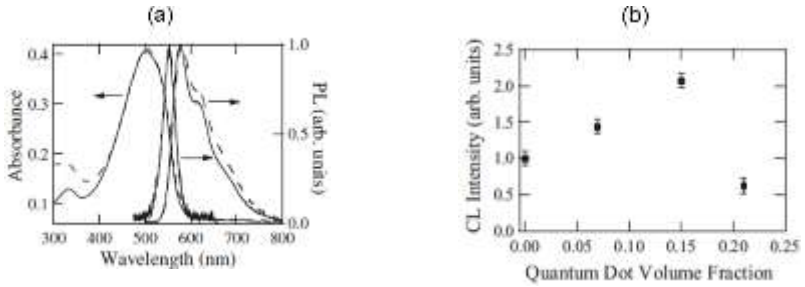

Figure 22. (a) Absorption and PL spectrum of MEH-PPV film (solid) and MEH-PPV QD 0.15 doped film (dashed) (b) CL intensity as a function of QD volume fraction (reproduced with permission from ref 79. Copyright 2006 WILEY-VCH).

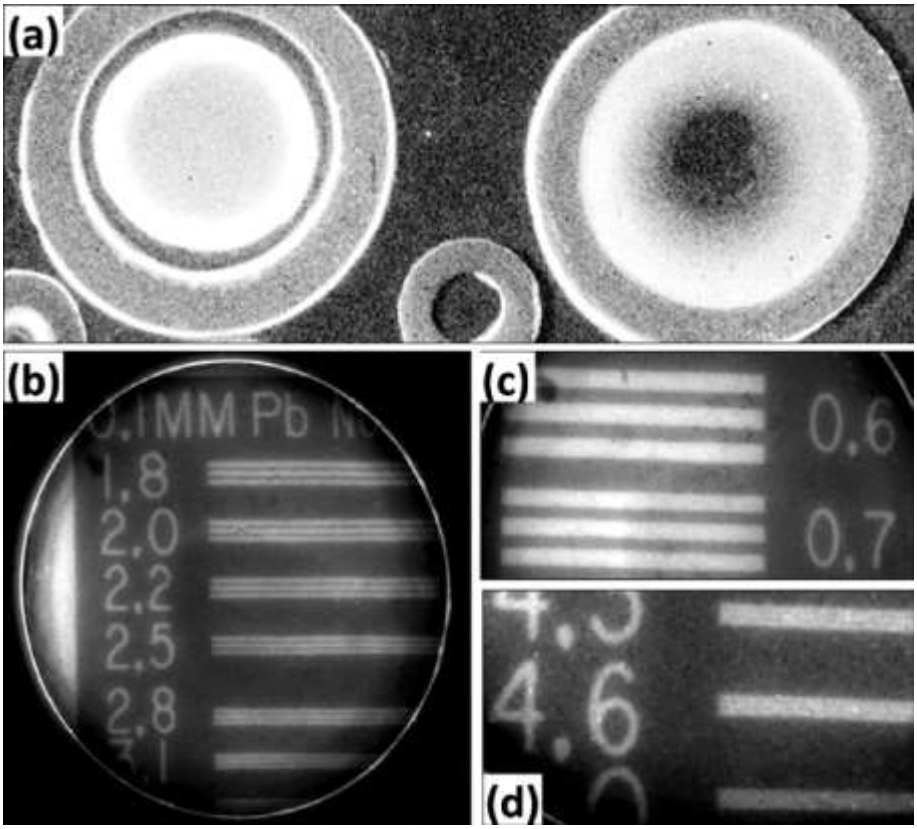

Figure 23. (a) X-ray image of CdTe and CdSe QD solution samples in containers (left: CdTe; right: CdSe). [(b)–(d)] X-ray imaging resolution study on a CdTe/PVA nanocomposite film; a 0.1 mm thick Pb mask was used; (b) area with resolution of 1.8–3.1 lines/mm; (c) low resolution area with 0.6 lines/mm; (d) enlarged image of higher resolution area with 4.3–5.0 lines/mm (reproduced with permission from ref 81. Copyright 2011 American Institute of Physics).

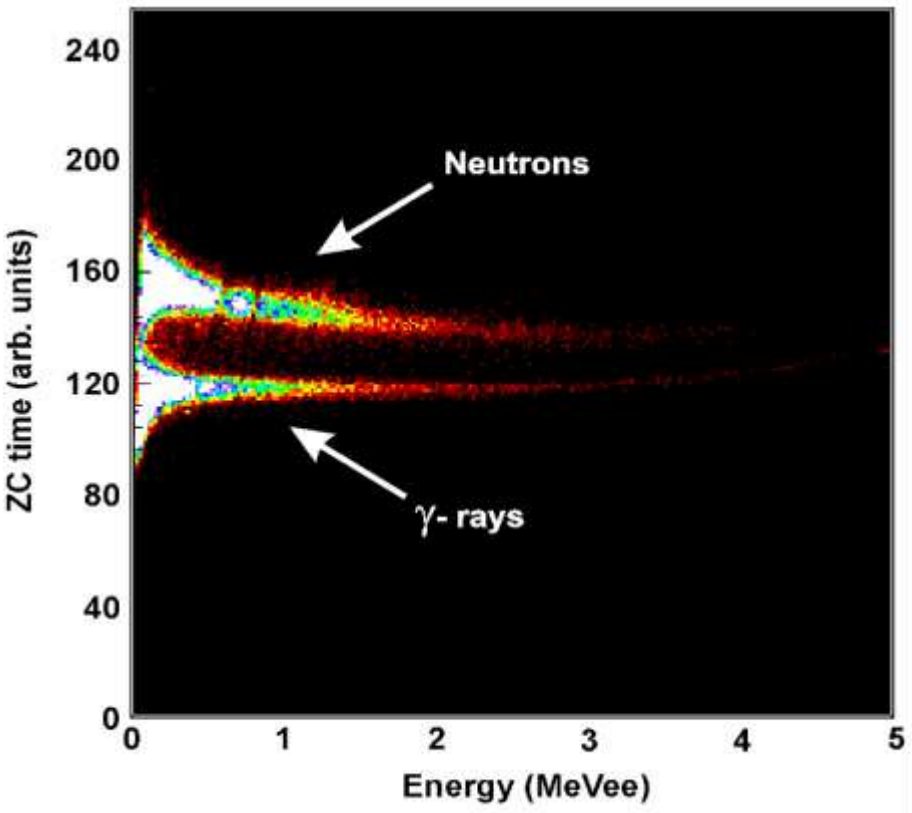

Figure 24. 2D plot of zero crossing time *vs*. energy measured with composite *p*-terphenyl based scintillator (50 × 25 mm) under irradiation of a shielded PuBe source (reproduced with permission from ref 84c. Copyright 2012 IOP Publishing).

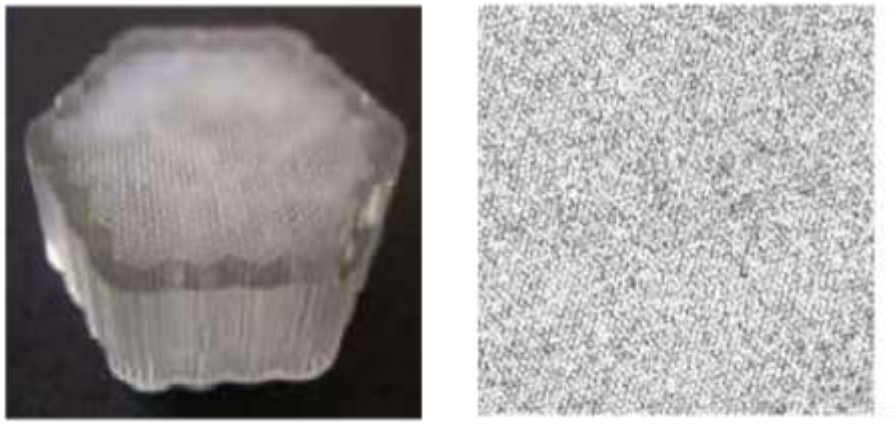

Figure 25. Left: Photographs of the capillary arrays; Right: A partial image (8 mm × 8 mm) of a capillary array illuminated by neutrons (reproduced with permission from ref 86b. Copyright 2007 IEEE).

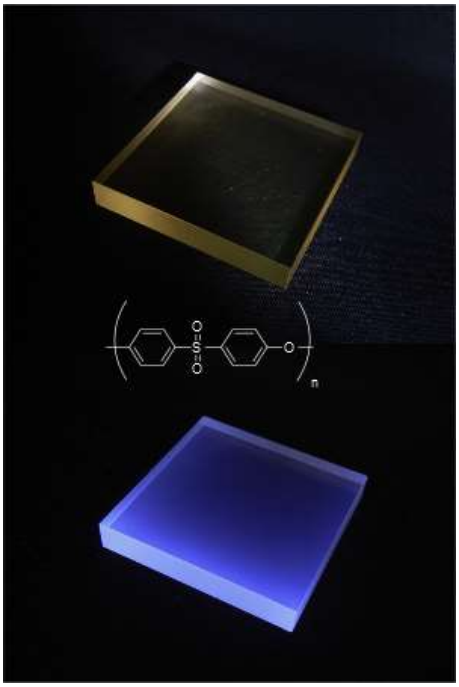

Figure 26. A 31× 31 × 5 mm poly(ether sulfone) plate. PES is an amber-coloured transparent resin (top) and under ultra-violet light (bottom) (reproduced with permission from ref 90. Copyright 2013 Elsevier B. V.).

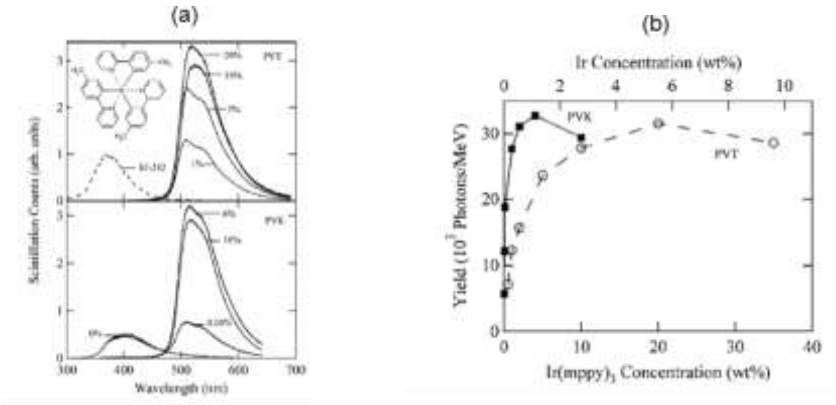

Figure 27. (a) Scintillation response as a function of wavelength for PVT (upper panel) and PVK (lower panel) incorporating the indicated weight percentages of Ir(mppy)$_3$; (b) Integrated scintillation yield for PVT (open circles) and PVK (solid squares) plastics as a function of Ir(mppy)$_3$ wt% (bottom axis) and Ir wt% (top axis) (reproduced with permission from ref 92. Copyright 2007 American Institute of Physics).

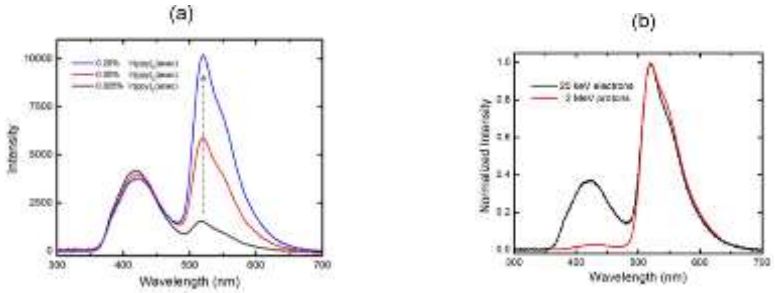

Figure 28. (a) Unnormalized cathodoluminescence spectra for PVK samples doped with 0.025 %, 0.05 %, and 0.20 wt% of Ir(ppy)$_2$(acac); (b) Steady-state cathodoluminescence and proton radioluminescence spectra for PVK doped with 0.2 wt% of Ir(ppy)$_2$(acac). The spectra are normalized to the maximum intensity peak at 515 nm to highlight the particle-specific response (reproduced with permission from ref 93b. Copyright 2012 IEEE).

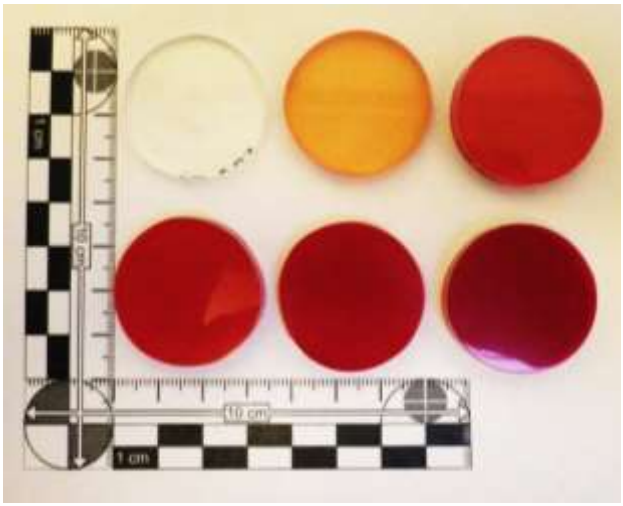

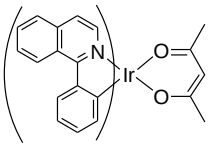

$Ir(piq)_2(acac)$

Figure 29. Cross-linked scintillators with increasing loading of $Ir(piq)_2(acac)$ (0 – 0.1 wt%).

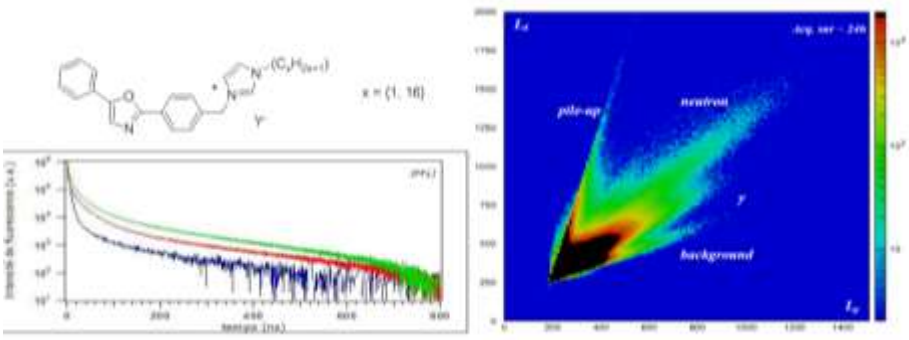

Figure 30. Top left: general structure of ionic liquids allowing PSD between fast neutrons and gamma; bottom left: scintillation decay profiles of *OxImC*$_{16}$-*PF*$_6$ (x = 16; Y = PF_6) under gamma excitation (blue), 2 MeV protons (red) and 2 MeV alphas (green). Right: example of PSD biparametric spectrum obtained from the same compound (reproduced with permission from ref 98b. Copyright 2011 from the Author).

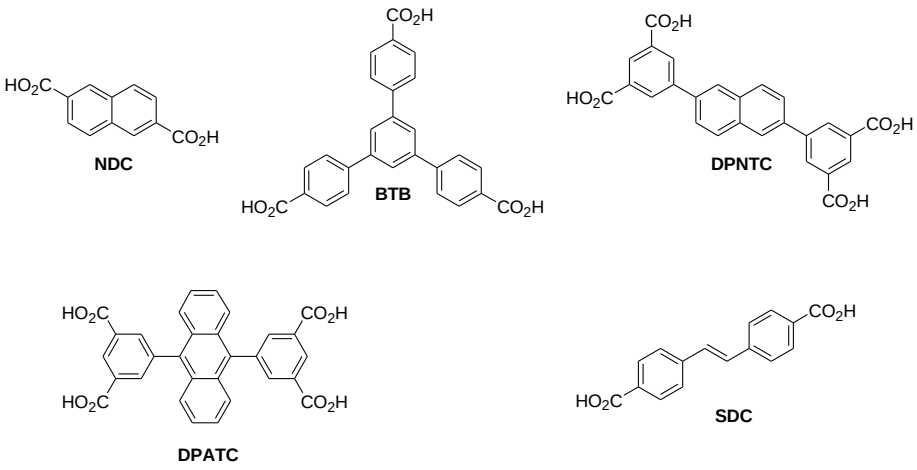

Figure 31. **Organic scintillators carboxylate derivatives used to build the MOFs.**

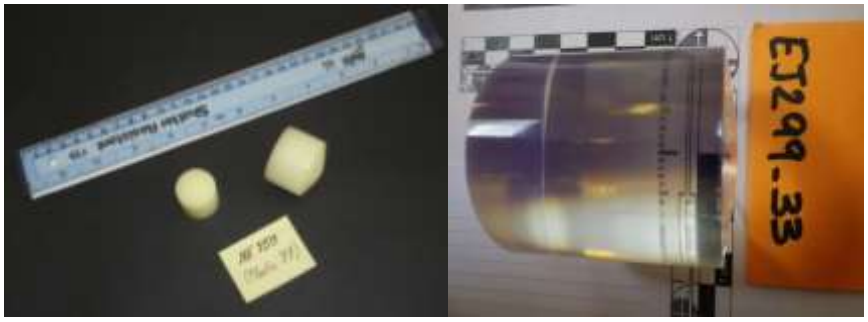

Figure 32. Pictures of NE-150 (left) and EJ-299-33 (right) after whitening and/or dishing of the morphology (Copyright F. Brooks for left picture, Copyright CEA for right picture).

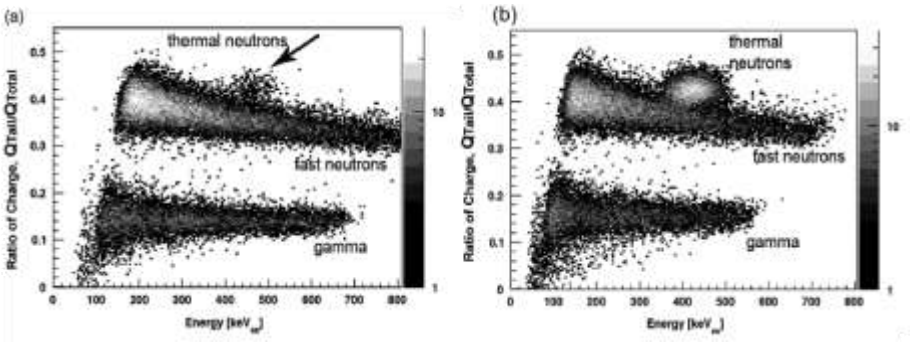

Figure 33. ^{252}Cf PSD patterns obtained with Li-loaded PSD plastics: (a) 5% of ^{Nat}Li-3-PSA (containing ≈ 0.01% of natural abundance ^{6}Li), 9 mm HDPE moderation; (b) 5% of ^{6}Li-3-PSA with 9 mm HDPE moderation (reproduced with permission from ref 106b. Copyright 2013 Elsevier B. V.).

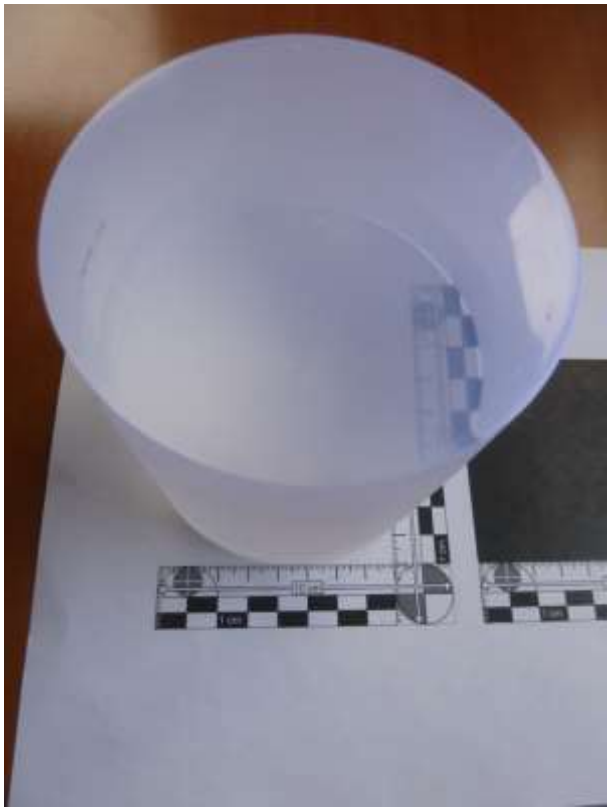

Figure 34. Picture of highly concentrated fluorophore, large plastic scintillator for n/γ discrimination (dimensions Ø 103 mm × h 114 mm, copyright 2013 CEA).

Table 1. Metals and specific isotopes that are potentially target for plastic scintillation applications.[44]

Elements / Isotopes	Applications
^{6}Li, ^{10}B, ^{113}Cd, ^{155}Gd, ^{157}Gd	Neutron detectors, searching for neutrinos oscillations
^{176}Yb, ^{160}Gd, ^{100}Mo, ^{37}Cl	Detection of solar neutrinos
Pb	Detection of astrophysics neutrinos
^{19}F, ^{73}Ge	Searching for Dark matter
^{150}Nd, ^{160}Gd, ^{100}Mo, ^{130}Te, ^{82}Se	Searching for double β decay
Pb, Sn, W, Hg, Bi	High energy physics

Table 2. Isotopes used for neutron capture.[108]

Isotopes	Thermal Cross section (Barns)	Natural abundance
^{6}Li	940	7.5 %
^{10}B	2,000	19.9 %
^{113}Cd	30,000	12.2 %
^{155}Gd	60,700	14.8 %
^{157}Gd	254,000	15.6 %

Table 3. Various sol-gel scintillators with dopants, fluorophores and characteristics.

Ref.	Loading elements	Fluorophores	Typical morphology	Comments
[109]	^{6}LiOH·H_2O $B(OH)_3$ $^{10}B(OH)_3$ $^{11}B(OH)_3$	Salicylic acid PPO POPOP	Ø 25.4 mm h < 1 mm	Two series produced. One “standard” and one doped with PEG-400.
[110]	Gd	Europium complex	n.d.	High density (7.1 g/cm^3)
[111]	^{6}Li- salicylate	PPO/POPOP as scintillation cocktail	Cylindrical monolith Dimension n.d.	Hybrid organic-inorganic material
[112]	^{6}LiOH·H_2O	Various	Ø 25.4 mm h ≈ 100’s µm	Study of various fluorophores
[113]	$B(OMe)_3$	Butyl-PBD	Ø ≈ 25 mm h ≈ mm	Doped with PEG
[114]	-	Europium complex	n.d.	Linear response up to 400 Gy
[115]	-	Carbon quantum dots	8 – 700 µm Xerogel	Thin films or bulk sizes

Table 4. Luminescence properties of MOFs.

Entry	Linker	PL_{ex} (nm)	PL_{em} (nm)	CL_{em} (nm)	Stokes Shift (nm)	τ_{PL} (ns)	τ_{cL} (ns)	Relative CL intensity
1	NDC/BTB	364	381	390	26	15 (100%)	15	0.79[a]

2	NDC	361	380	425	64	11 (100%)	11	1.24[a]
3	NDC	365	384	440	75	11 (98%) 1 (2%)	8	0.55[a]
4	DPNTC	353	381	410	57	11 (92%) 4 (8%)	11	0.64[a]
5	DPATC	397	438	475	78	1 (86%) 514 (%)	3	0.39[a]
6	SDC	375	390	474	99	n.d.	n.d.	0.09[b]
7	SDC	410	441	449	39	n.d.	n.d.	0.22[b]

(a) relative to *trans*-stilbene crystals
(b) relative to anthracene crystals

Table 5. Composition of the polystyrene PPO/QD based scintillators.

Sample	PPO	CdSe Quantum Dots	x-ray induced fluorescence intensity (arb. u.)
PS	-	-	5
PS/PPO	0.2 %	-	4
PS/QD	-	0.2 %	7
PS/PPO/QD	0.2 %	0.2 %	23

Table 6. Composition and scintillation properties of the samples.

Sample	Matrix	Fluorophore	$BiPh_3$	Relative gamma yield at 662 keV	Resolution FWHM at 662 keV
1a	PVK	3% DPA	40%	0.66	9%
2a	PVK	3% FIrpic	40%	0.78	6.8%
2c	PVK	3% FIrpic	-	0.73	9%
EJ-208	PVT	Unknown	-	1	8%

Table 7. Different strategies and results for neutron/gamma discrimination in plastic scintillators.

Ref.	Strategy	Biggest size (Ø, h)	FOM (at given energy)	Scintillation yield (ph/MeV)	Decay time (ns)	Emission wavelength (nm)	Source	Comments
83c	Stilbene single crystals in silicone	200 mm × 20 mm	1.00 (500 keVee)	n.d.	4.5 (assumption)	410 (assumption)	^{252}Cf	-
84b	*p*-T or stilbene single crystals in Sylgard	50 mm × 50 mm	1.41 (*p*-T, 600 keVee) 1.19 (stilbene, 600 keVee)	≈ 9,900 (*p*-T) ≈ 5,700 (stilbene)	n.d.	420 (*p*-T); 395 (stilbene)	10 cm Pb-shielded 500 mCi PuBe	Diffusion issues which lowers performances for big samples
101	1st fluo highly concentrated	25 mm × 25 mm	n.d.	n.d.	n.d.	≈ 420 (assumption	PoBe	Ageing and whitening

						)		
102e	1st fluo highly concentrated	103 mm × 114 mm	0.69 (38 × 38 mm, 200 keVee)	3,400	13	420	AmBe	Low scintillation yield
103b	1st fluo highly concentrated	50 mm × 50 mm	3.31 (25 × 25 mm, 480 keVee)	n.d.	n.d.	≈ 430	5.1 cm Pb-shielded ^{252}Cf	Precursor of EJ-299-33 (see line below)
104	EJ-299-33	127 mm × 150 mm	-	8,600	n.d.	420	-	From commercial brochure
105c	EJ-299-33	50 mm × 50 mm	≈ 0.8 (200 keVee)	8,600	n.d.	420	^{252}Cf	-
11	1st fluo highly concentrated	100 cm^3	1.6 (500 keVee)	Up to 13,000 (size-dependent)	6.0 – 9.5 ns ([PPO]-dependent)	385 – 440 ([PPO]-dependent)	AmBe	Similar to [103b]
93b	Organometallics	25 mm × 15 mm	1.4 (400 keVee)	7,300	800	515	AmBe	Elevated cost?
94b	Organometallics	16 mm × 10 mm	1.37 (250 keVee)	n.d.	370,000	590 – 620	1 cm Pb-shielded PuBe	Independent from TTA
98	Ionic liquids	Micrometers	n.d.	n.d.	< 50 (assumption)	≈ 380 (assumption)	AmBe	Currently limited to small sizes only
17d	Polysiloxanes	30 mm × 10 mm	n.d.	4,000	n.d.	610	n.d.	-

Note: some references refer to the first published document, whereas some others refer to benchmark of scintillators. Ref 101 is added for better comparison.

Acknowledgements
S.G. is indebted to the grant allowed from the Agence Nationale de la Recherche. All the Authors contributed equally to this work.

Received: ((will be filled in by the editorial staff))
Revised: ((will be filled in by the editorial staff))
Published online: ((will be filled in by the editorial staff))

Copyright WILEY-VCH Verlag GmbH & Co. KGaA, 69469 Weinheim, Germany, 2013.

The table of contents entry should be 50–60 words long, and the first phrase should be bold. **Plastic scintillators are fluorescent polymers able to emit light while exposed to ionizing radiation**. Known since late 50's, their chemistry is gained a lot of interest this last decade. Recent developments are exposed.

Keyword
Plastic scintillators, polymers, fluorescence, dyes, nuclear instrumentation, radiation detector.

*Guillaume V.H. Bertrand, Fabien Sguerra and Matthieu Hamel**

Current status on plastic scintillators modifications

ToC figure

5. Bibliography

[1] http://www.iaea.org/newscenter/news/2013/mexicoradsource4.html (last access Jan 21st, 2014).

[2] Stromswold, D. C.; Siciliano, E. R.; Schweppe, J. E.; Ely, J. H.; Milbrath, B. D.; Kouzes, R. T.; Geelhood, B. D. *IEEE Nucl. Sci. Symp. Conf.* **2003**, *2*, 1065-1069.

[3] Schorr, M. G.; Torney, F. L. *Phys. Rev.* **1950**, *80*, 474.

[4] Brooks, F. D. *Nucl. Instr. Methods* **1979**, *162*, 477-505.

[5] Moser, S. W.; Harder, W. F.; Hurlbut, C. R.; Kusner, M. R. *Radiat. Phys. Chem.* **1993**, *41*, 31-36.

[6] Salimgareeva, V. N.; Kolesov, S. V. *Instr. Exp. Techn.* **2005**, *48*, 273-282.

[7] Aspler, J. S.; Hoyle, C. E.; Guillet, J. E. *Macromolecules* **1978**, *11*, 925–929

[8] Kallmann, H. P.; Furst, M.; Brown, F. H. American Patent Application US3068178, 1962

[9] Salimgareeva, V. N.; Polevoi, R. M.; Ponomareva, V. A.; Sannikova, N. S.; Kolesov, S. V.; Leplyanin, G. V. *Russ. J. Appl. Chem*. **2003**, *76*, 1655-1658.

[10] Inagaki, T.; Takashima, R. *Nucl. Instr. Methods* **1982**, *201*, 511-517.

[11] van Loef, E. V.; Markosyan, G.; Shirwadkar, U.; Shah, K. S. *IEEE Trans. Nucl. Sci*. **2014**, *61*, 467-471.

[12] Rebourgeard, P.; Rondeaux, F.; Baton, J. P.; Besnard, G.; Blumenfeld, H.; Bourdinaud, M.; Calvet, J.; Cavan, J.-C.; Chipaux, R.; Giganon, A.; Heitzmann, J.; Jeanney, C.; Micolon, P.; Neveu, M.; Pedrol, T.; Pierrepont, D.; Thévenin, J.-C. *Nucl. Instr. Methods A* **1999**, *427*, 543-567.

[13] (a) Bowen, M.; Majewski, S.; Pettey, D.; Walker, J.; Wojcik, R.; Zorn, K. *IEEE Trans. Nucl. Sci.* **1989**, *36*, 562-566; (b) Feygelman, V. M.; Walker, J. K.; Harmon, J. P. *Nucl. Instr. Methods A* **1990**, *295*, 94-98.

[14] Deshpande, G.; Rezac, M. E. *Polym. Degrad. Stab*. **2002**, *76*, 17-24.

[15] Patel, M.; Murphy, J. J.; Skinner, A. R.; Powell, S. J.; Smith, P. F. *Polym. Test.* **2003**, *22*, 923–928

[16] (a) Bell, Z. W.; Brown, G. M.; Ho, C. H.; Sloop, F. V *Proc. SPIE* **2002**, *4784*, 150-163; (b) Quaranta, A.; Carturan, S.; Marchi, T.; Cinausero, M.; Scian, C.; Kravchuk, V. L.; Degerlier, M.; Gramegna, F.; Poggi, M.; Maggioni, G. *Opt. Mater.* **2010**, *32*, 1317-1320.

[17] (a) Quaranta, A.; Carturan, S. M.; Marchi, T.; Kravchuk, V. L.; Gramegna, F.; Maggioni, G.; Degerlier, M. *IEEE Trans. Nucl. Sci.* **2010**, *57*, 891-900; (b) Quaranta, A.; Carturan, S.; Marchi, T.; Antonaci, A.; Scian, C.; Kravchuk, V. L.; Degerlier, M.; Gramegnac, F.; Maggioni, G. *Nucl. Instr. Methods B* **2010**, *268*, 3155-3159; (c) Quaranta, A.; Carturan, S.; Cinausero, M.; Marchi, T.; Gramegna, F.; Degerlier, M.; Cemmi, A.; Baccaro, S. *Mat. Chem. Phys.* **2013**, *137*, 951-958; (d) Dalla Palma, M.; Quaranta, A.; Marchi, T.; Collazuol, G.; Carturan, S.; Cinausero, M.; Gramegna, F. *IEEE proceedings of ANIMMA 2013* **2014**.

[18] Bell, Z. W.; Miller, M. A.; Maya, L.; Brown, G. M.; Sloop Jr., F. V. *IEEE Trans. Nucl. Sci.* **2004**, 1773-1776.

[19] Carturan, S.; Quaranta, A.; Marchi, T.; Gramegna, F.; Degerlier, M.; Cinausero, M.; Kravchuk, V. L.; Poggi, M. *Radiat. Prot. Dosim.* **2011**, *143*, 471-476.

[20] Quaranta, A.; Carturan, S.; Marchi, T.; Buffa, M.; Degerlier, M.; Cinausero, M.; Guastalla, G.; Gramegna, F.; Valotto, G.; Maggioni, G.; Kravchuk, V. L. *J. Non-Crystal. Solids* **2011**, *357*, 1921-1925.

[21] Beddar, A. S. *Radiat. Meas.* **2007**, *41*, S124-S133.

[22] http://www.epotek.com/site/administrator/components/com_products/assets/files/Style_Uploads/305.pdf (last access January 31st, 2014).

[23] Markley, F. W. *Mol. Cryst.* **1968**, *4*, 303-317.

[24] Kang, Z.; Barta, M.; Nadler, J.; Wagner, B.; Rosson, R.; Kahn, B. *J. Lumin.* **2011**, *131*, 2140-2143.

[25] McElhaney, S. A.; Chiles, M. M.; Ramsey, J. A. *IEEE Nucl. Sci. Symp. Conf. Rec.* **1990**, 425-428.

[26] Lindvold, L. R.; Beierholm, A. R.; Andersen, C. E. *Radiat. Meas.* **2010**, *45*, 615–617.

[27] Nakamura, H.; Kitamura, H.; Hazama, R. *Proc. R. Soc. A* **2010**, *466*, 2847-2859.

[28] Nakamura, H.; Shirakawa, Y.; Takahashi, S.; Shimizu, H. *Europhys. Lett.* **2010**, *95*, 22001.

[29] (a) Nakamura, H. ; Shirakawa, Y.; Kitamura, H.; Yamada, T.; Shidara, Z.; Yokozuka, T.; Nguyen, P.; Takahashi, T.; Takahashi, S. *Radiat. Meas.* **2013**, *59*, 172-175; (b) Nakamura, H.; Yamada, T.; Shirakawa, Y.; Kitamura, H.; Shidara, Z.; Yokozuka, T.; Nguyen, P.; Kanayama, M.; Takahashi, S. *Appl. Radiat. Isot.* **2013,** *80*, 84-87.

[30] (a) Saito, M.; Nishiyama , F.; Kobayashi , K.; Nagata, S.; Takahiro K. *Nucl. Instrum. Methods B* **2010**, *268*, 2918-2922; (b) Nagata, S.; Katsui, H.; Takahiro, K.; Tsuchiya, B.; Shikama, T. *Nucl. Instrum. Methods B* **2010**, *268*, 3099-3102; (c) Nagata ,S.; Mitsuzuka , M.; Onodera , S.; Yaegashi , T.; Hoshi , K.; Zhao, M.; Shikama, T. *Nucl. Instrum. Methods B* **2013**, *315*, 157-160.

[31] Sen, I.; Urffer, M.; Penumadu, D.; Young, S. A.; Miller, L. F.; Mabe, A. N. *IEEE Trans. Nucl. Sci.* **2012**, *59*, 1781-1786.

[32] Quaranta, A.; Carturan, S.; Maggioni, G.; Milazzo, P. M.; Abbondanno, U.; Della Mea, G.; Gramegna, F.; Pieri, U. *IEEE Trans. Nucl. Sci.* **2001**, *48*, 219-224.

[33] (a) Quaranta, A.; Vomiero, A.; Carturan, S.; Maggioni, G.; Mea, G. D. *Synth. Met.* **2003**, *138*, 275-279; (b) Carturan, S.; Quaranta, A.; Vomiero, A.; Bonafini, M.; Maggioni, G.; Della Mea, G. *IEEE Nucl. Sci. Symp. Conf.* **2004**, *2*, 869-873; (c) Carturan, S.; Quaranta, A.; Vomiero, A.; Bonafini, M.; Maggioni, G.; Della Mea, G. *IEEE Trans. Nucl. Sci.* **2005**, *52*, 748-751; (d) Quaranta, A. *Nucl. Instr. Methods A* **2005**, *240*, 117-123.

[34] Rutkowska, M.; Eisenberg, A. *J. Appl. Polym. Sci.* **1985**, *30*, 3317-3323.

[35] Breukers, R. D.; Bartle, C. M.; Edgar, A. *Nucl. Instr. Methods A* **2013**, *701*, 58-61.

[36] Britvich, G. I.; Vasil'chenko, V. G.; Lishin, V. A.; Polyakov, V. A.; Solov'ev, A. S. *Instr. Exp. Techn*. **2001**, *44*, 472-484.

[37] Menaa, N.; Villani, M.; Croft, S.; McElroy, R. B.; Philips, S. A.; Czirr, J. B. *IEEE Trans. Nucl. Sci.* **2009**, *56*, 911-914.

[38] (a) Williams, A. M.; Beeley, P. A.; Spyrou, N. M. *Radiat. Prot. Dosim.* **2004**, *110*, 497-502; (b) Lewis, D. V; Spyrou, N. M.; Williams, A. M.; Beeley, P. A. *Radiat. Prot. Dosim.* **2007**, *126*, 390-393.

[39] Czirr, J. B.; Merrill, D. B.; Buehler, D.; McKnight, T. K.; Carroll, J. L.; Abbott, T.; Wilcox, E. *Nucl. Instr. Methods A* **2002**, *476*, 309-312.

[40] Shestakova, I.; Ovechkina, E.; Gaysinskiy, V.; Antal, J. J.; Bobek, L.; Nagarkar, V. *IEEE Trans. Nucl. Sci.* **2007**, *54*, 1797-1800.

[41] Sytnik, O. U.; Svidlo, O. V.; Zhmurin, P. N. *Funct. Mater*. **2013**, *20*, 243-247.

[42] Bross, A. D.; Mellott, K. L.; Pla-Dalmau, A. Amercian Patent Application US2004104500, 2004.

[43] (a) Normand, S.; Mouanda, B.; Haan, S.; Louvel, M. *Nucl. Instr. Methods A* **2002**, *484*, 342-350; (b) Normand, S.; Mouanda, B.; Haan, S.; Louvel, M. *IEEE Trans. Nucl. Sci.* **2002**, *49*, 1603-1608; (c) Normand, S.; Delacour, P.; Passard, C.; Loridon, J. *IEEE Symp. Conf. Rec. Nucl. Sci.* **2004**, *2*, 787-789.

[44] Brudanin, V. B.; Bregadze, V. I.; Gundorin, N. A.; Filossofov, D. V; Kochetov, O. I.; Nemtchenok, I. B.; Smolnikov, A. A.; Vasiliev, S. I. In *Identif. Dark Matter, Proc. Int. Workshop, 3rd*; 2001; pp. 626-634.

[45] Ishikawa, M.; Ono, K.; Sakurai, Y.; Unesaki, H.; Uritani, A.; Bengua, G.; Kobayashi, T.; Tanaka, K.; Kosako, T. *Appl. Radiat. Isot.* **2004**, *61*, 775-779.

[46] Bell, Z. W.; Brown, G. M.; Ho, C. H.; Sloop, F. V. *Proc. SPIE* **2002**, *4784*, 150–163.

[47] Nemchenok, I. B.; Gundorin, N. A.; Shevchik, E. A.; Shurenkova, A. A. *Funct. Mater.* **2013**, *3*, 310-313

[48] Velmozhnaya, E. S.; Bedrick, A. I.; Zhmurin, P. N.; Titskaya, V. D.; Adadurov, A. F.; Sofronov, D. S. *Funct. Mater.* **2013**, *4*, 494-499

[49] Ovechkina, L.; Riley K.; Miller, S.; Bell, Z.; Nagarkar, V. *Phys. Procedia* **2009,** *2*, 161–170.

[50] Bedrik, A. I.; Velmozhnaya, E. S.; Zhmurin, P. N.; Adadurov, A. F.; Lebedev V. N.; Titskaya, V. D. *Funct. Mater.* **2011**, *4*, 470-475

[51] Cai, W.; Chen, Q.; Cherepy, N.; Dooraghi, A.; Kishpaugh, D.; Chatziioannou, A.; Payne, S.; Xiang, W.; Pei, Q. *J. Mater. Chem. C* **2013**, *1*, 1970-1976.

[52] Sen, I.; Penumadu, D.; Williamson, M.; Miller, L. F.; Green, A. D.; Mabe, A. N. *IEEE Trans. Nucl. Sci.* **2011**, *58*, 1386-1393.

[53] Uppal, R.; Sen, I.; Penumadu, D.; Young, S. A.; Urffer, M. J.; Miller, L. F. *Adv. Eng. Mater*. **2014**, *16*, 196-201.

[54] Mabe, A. N.; Auxier, J. D. I.; Urffer, M. J.; Penumadu, D.; Schweitzer, G. K.; Miller, L. F. *Nucl. Instr. Methods A* **2013**, *722*, 29-33.

[55] Britvich, G. I.; Vasil'chenko, V. G.; Lapshin, V. G.; Solov'ev, A. S. *Instr. Exp. Techn*. **2000**, *43*, 36-39.

[56] (a) Hamel, M.; Darbon, S.; Normand, S.; Turk, G. French Patent Application FR1060977, 2010; (b) Turk, G.; Reverdin, C.; Gontier, D.; Darbon, S.; Dujardin, C.; Ledoux, G.; Hamel, M.; Simic, V.; Normand, S. *Rev. Sci.*

Instrum. **2010**, *81*, 10E509; (c) Hamel, M.; Simic, V.; Normand, S.; Turk, G.; Darbon, S. *In* LSC 2010, Advances in Liquid Scintillation Spectrometry Paris, **2011**, p 291-296; (d) Hamel, M.; Turk, G.; Rousseau, A.; Darbon, S.; Reverdin, C.; Normand, S. *Nucl. Instr. Methods A* **2011**, *660*, 57-63; (e) Hamel, M.; Normand, S.; Turk, G.; Darbon, S. *IEEE proceedings of ANIMMA 2011*, **2012**; (f) Hamel, M.; Normand, S.; Turk, G.; Darbon, S. *IEEE Trans. Nucl. Sci*. **2012**, *59*, 1268-1272; (g) Hamel, M.; Dehé-Pittance, C.; Coulon, R.; Carrel, F.; Pillot, P.; Barat, E.; Dautremer, T.; Montagu, T.; Normand, S. *IEEE Proceedings of ANIMMA 2013*, **2014**.

[57] Rousseau, A. "Développement d'un imageur à rayons X durci pour l'environnement radiatif du Laser Mégajoule", PhD Thesis, École polytechnique, France, 2014.

[58] (a) Rousseau, A.; Darbon, S.; Girard, S.; Paillet, P.; Bourgade, J.-L.; Goiffon, V.; Magnan, P.; Lalucaa, V.; Hamel, M.; Larour, J. *Proc. SPIE* **2012**, *8439*, 84391F; (b) Rousseau, A.; Darbon, S.; Paillet, P.; Girard, S.; Bourgade, J. L.; Raine, M.; Duhamel, O.; Goiffon, V.; Magnan, P.; Chabanne, A.; Cervantes, P.; Hamel, M.; Larour, J. *Proc. SPIE* **2013**, *8850*, 885004; (c) Rousseau, A.; Darbon, S.; Troussel, P.; Caillaud, T.; Bourgade, J. L.; Turk, G.; Vigne, E.; Hamel, M.; Larour, J.; Bradley, D.; Smalyuk, V.; Bell, P. *EPJ Web Conf.* **2013**, *59*, 13006.

[59] Dzhardimalieva, G. I.; Pomogailo, A. D. *Russ. Chem. Rev.* **2008**, *77*, 259-301.

[60] (a) Cherepy, N. J.; Sanner, R. D.; Payne, S. A.; Rupert, B. L.; Sturm, B. W. PCT Patent Application WO2012044379, 2010; (b) Cherepy, N. J.; Payne, S. A.; Sturm, B. W.; Kuntz, J. D.; Seeley, Z. M.; Rupert, B. L.; Sanner, R. D.; Drury, O. B.; Hurst, T. A.; Fisher, S. E.; Groza, M.; Matei, L.; Burger, A.; Hawrami, R.; Shah, K. S.; Boatner, L. A. *IEEE Nucl. Sci. Symp. Conf.* **2010**, 1288-1291; (c) Rupert, B. L.; Cherepy, N. J.; Sturm, B. W.; Sanner, R. D.; Dai, Z.; Payne, S. A. "Bismuth-Loaded Polymer Scintillators for Gamma Ray Spectroscopy," LLNL, 2011; (d) Rupert, B. L.; Cherepy, N. J.; Sturm, B. W.; Sanner, R. D.; Payne, S. A. *Europhys. Lett.* **2012**, *97*, 22002.

[61] Fritsch, J.; Mansfeld, D.; Mehring, M.; Wursche, R.; Grothe, J.; Kaskel, S. *Polymer* **2011**, *52*, 3263-3268.

[62] Bertrand, G. H. V.; Sguerra, F.; Hamel, M.; Dehé-Pittance, C.; Pillot, P.; Coulon, R.; Carrel, F.; Barat, É.; Dautremer, T.; Montagu, T.; Normand, S. *J. Mater. Chem. C* **2014**, *Submitted*.

[63] Shmurak, S. Z.; Kedrov, V. V.; Klassen, N. V.; Shakhrai, O. A. *Phys. Solid State* **2012**, *54*, 2266-2276.

[64] Blanc, P.; Sibczyński, P.; Iwanowska, J.; Carrel, F.; Hamel, M.; Syntfeld-Każuch, A.; Normand, S. *Nucl. Instr. Methods A* **2014**, *Submitted*.

[65] Britvich, I. G.; Vasil'chenko, V. G.; Kirichenko, V. N.; Kuptsov, S. I.; Lapshin, V. G.; Soldatov, A. P.; Solov'ev, A. S.; Rykalin, V. I.; Chernichenko, S. K.; Shein, I. V. *Instr. Exp. Techn*. **2002**, *45*, 644-654.

[66] Simonetti, J. J.; Ziegler, W. P.; Durner Jr., E. F.; Busser, C. D. M. French Patent Application FR2844885, 2003.

[67] (a) Hamel, M.; Rocha, L.; Pittance, C.; Trocmé, M. French Patent Application FR2983310, 2011; (b) Kondrasovs, V.; Boudergui, K.; Normand, S.; Hamel, M.; Rocha, L.; Pittance, C.; Trocmé, M. French Patent Application FR2983311, 2011.

[68] Hamel, M.; Normand, S.; Simic, V. *React. Funct. Polym.* **2008**, *68*, 1671-1681.

[69] O'Bryan, G.; Vance, A. L.; Mrowka, S.; Mascarenhas, N. *Final LDRD Report: Advanced Plastic Scintillators for Neutron Detection*; Sandia National Laboratories, 2010; p. 16.

[70] Adadurov, A. F.; Yelyseev, D. A.; Titskaya, V. D.; Lebedev, V. N.; Zhmurin, P. N. *Radiat. Meas.* **2011**, *46*, 498-502.

[71] (a) Frahn, M. S.; Luthjens, L. H.; Warman, J. M. *Polymer* **2003**, *44*, 7933-7938; (b) Frahn, M. S.; Luthjens, L. H.; Warman, J. M. *J. Phys. Chem. B* **2004**, *108*, 2839-2845.

[72] (a) Hamerton, I.; Hay, J. N.; Jones, J. R.; Lu, S.-Y. *LSC 2001, Advances in Liquid Scintillation Spectrometry* **2001**, 137-139; (b) Hamerton, I.; Hay, J. N.; Jones, J. R.; Lu, S.-Y. *Chem. Mater*. **2000**, *12*, 568-572.

[73] (a) Pla-Dalmau, A.; Bross, A. D.; Mellott, K. L. *Nucl. Instr. Methods A* **2001**, *466*, 482–491; (b) Pla-Dalmau, A.; Bross, A. D.; Rykalin, V. V. *IEEE Nucl. Sci. Symp. Conf.* **2003**, *1*, 102-104; (c) Pla-Dalmau, A.; Bross, A. D.; Rykalin, V. V.; Wood, B. M. *IEEE Nucl. Sci. Symp. Conf.* **2005**, *3*, 1298-1300.

[74] Vasil'chenko, V. G.; Kirichenko, V. N.; Soldatov, A. P.; Chernichenko, S. K. *Instr. Exp. Techn.* **2003**, *46*, 467-476.

[75] Sótér, A.; Todoroki, K.; Kobayashi, T.; Barna, D.; Horváth, D.; Hori M. *Rev. Sci. Instrum.* **2014**, *85*, 023302.

[76] Tomczak, N.; Jańczewski, D.; Han, M.; Vancso, G. J. *Prog. Polym. Sci.* **2009**, *34*, 393-430.

[77] (a) Létant, S. E.; Wang, T.-F. *Appl. Phys. Lett.* **2006**, *88*, 103110; (b) Létant, S. E.; Wang, T.-F. *Nano Lett.* **2006**, *6*, 2877-2880.

[78] Rogers, T.; Han, C.; Wagner, B.; Nadler, J.; Kang, Z. *MRS Online Proc. Libr.* **2011**, *1312*, 355-360.

[79] Campbell, I. H.; Crone, B. K. *Adv. Mater.* **2006**, *18*, 77-79.

[80] Park, J. M.; Kim, H. J.; Hwang, Y. S.; Kim, D. H.; Park, H. W. *J. Lumin.* **2014**, *146*, 157-161.

[81] Kang, Z.; Zhang, Y.; Menkara, H.; Wagner, B. K.; Summers, C. J.; Lawrence, W.; Nagarkar, V. *Appl. Phys. Lett.* **2011**, *98*, 181914.

[82] (a) Lawrence, W. G.; Thacker, S.; Palamakumbura, S.; Riley, K. J.; Nagarkar, V. V. *IEEE Nucl. Sci. Symp. Conf. Rec.* **2010**, 242-252; (b) Lawrence, W. G.; Thacker, S.; Palamakumbura, S.; Riley, K. J.; Nagarkar, V. V *IEEE Trans. Nucl. Sci.* **2012**, *59*, 215-221.

[83] (a) Budakovsky, S. V.; Galunov, N. Z.; Grinyov, B. V.; Karavaeva, N. L.; Kim, J. K.; Kim, Y.-K.; Pogorelova, N. V.; Tarasenko, O. A. *Radiat. Meas*. **2007**, *42*, 565-568; (b) Budakovsky, S. V.; Galunov, N. Z.; Karavaeva, N. L.; Kim, J. K.; Kim, Y. K.; Tarasenko, O. A.; Martynenko, E. V. *IEEE Trans. Nucl. Sci*. **2007**, *54*, 2734-2740; (c) Budakovsky, S. V.; Galunov, N. Z.; Grinyov, B. V.; Kim, J. K.; Kim, Y. K.; Tarasenko, O. A. *Funct. Mater*. **2009**, *16*, 86-91; (d) Karavaeva, N. L.; Tarasenko, O. A. *Funct. Mater*. **2009**, *16*, 92-96; (e) Galunov, N. Z.; Grinyov, B. V.; Karavaeva, N. L.; Kim, J. K.; Kim, Y. K.; Tarasenko, O. A.; Martynenko, E. V. *IEEE Trans. Nucl. Sci*. **2009**, *56*, 904-910; (f) Karavaeva, N. L.; Taras, O. A. *Funct. Mater*. **2010**, *17*, 379-385; (g) Tarasenko, O.; Galunov, N.; Karavaeva, N.; Lazarev, I.; Panikarskaya, V. *Radiat. Meas*. **2013**, *58*, 61-65; (h) Lee, S. K.; Son, J. B.; Jo, K. H.; Kang, B. H.; Kim, G. D.; Seo, H.; Park, S. H.; Galunov, N. Z.; Kim, Y. K. *J. Nucl. Sci. Technol*. **2014**, *51*, 37-47.

[84] (a) Iwanowska, J.; Moszynski, M.; Swiderski, L.; Syntfeld-Kazuch, A.; Szczesniak, T.; Sibczynski, P.; Galunov, N. Z.; Karavaeva, N. L. *IEEE Nucl. Sci. Symp. Conf. Rec.* **2009**, *N25-90*, 1437-1440; (b) Iwanowska, J.; Swiderski, L.; Moszynski, M.; Szczesniak, T.; Sibczynski, P.; Galunov, N. Z.; Karavaeva, N. L. *J. Instrum.* **2011**, *6*, P07007; (c) Iwanowska, J.; Swiderski, L.; Moszynski, M. *J. Instrum.* **2012**, *7*, C04004.

[85] Karavaeva, N. L.; Galunov, N. Z.; Martynenko, E. V.; Kosinova, A. V. *Funct. Mater*. **2010**, *17*, 549-553.

[86] (a) Nagarkar, V.; Sheshtakova, I.; Ovechkina, L. American Patent Application US7372041, 2007; (b) Shestakova, I.; Ovechkina, E.; Gaysinskiy, V.; Antal, J. J.; Bobek, L.; Nagarkar, V. *IEEE Trans. Nucl. Sci*. **2007**,

54, 1797-1800; (c) Riley, K. J.; Ovechkina, L.; Palamakumbura, S.; Bell, Z.; Miller, S.; Nagarkar, V. V. *IEEE Nucl. Sci. Symp. Conf. Rec.* **2010**, 1777-1780.

[87] Disdier, L.; Fedotoff, A. PCT Patent Application WO03081279, 2003.

[88] Santiago, L. M.; Bagán, H.; Tarancón, A.; Garcia, J. F. *Nucl. Instr. Methods A* **2013**, *698*, 106-116.

[89] Osakada, Y.; Pratx, G.; Hanson, L.; Solomon, P. E.; Xing, L.; Cui, B. *Chem. Commun*. **2013**, *49*, 4319-4321.

[90] Nakamura, H.; Shirakawa, Y.; Kitamura, H.; Sato, N.; Takahashi, S. *Appl. Radiat. Isot*. **2014**, *86*, 36-40.

[91] Yersin, H. *Top. Curr. Chem.*, **2004**, *24*, 1-26.

[92] Campbell, I. H.; Crone, B. K. *Appl. Phys. Lett.* **2007**, *90*, 12117.

[93] (a) Doty, F. P.; Allendorf, M. D.; Feng, P. L. PCT Patent Application WO2011/060085, 2011; (b) Feng, P. L.; Villone, J.; Hattar, K.; Mrowka, S.; Wong, B. M.; Allendorf, M. D.; Doty, F. P. *IEEE Trans. Nucl. Sci.* **2012**, *59*, 3312-3319.

[94] (a) Zhmurin, P. N.; Lebedev, V. N.; Adadurov, A. F.; Pereymak, V. N.; Gurkalenko, Y. A. *Funct. Mater*. **2013**, *20*, 500-503; (b) Zhmurin, P. N.; Lebedev, V. N.; Adadurov, A. F.; Pereymak, V. N.; Gurkalenko, Y. A. *Radiat. Meas*. **2014**, *62*, 1-5.

[95] Sguerra, F.; Bertrand, G. H. V.; Coulon, R.; Marion, R.; Sauvageot, E.; Daniellou, R.; Renaud, J.-L.; Normand, S.; Gaillard, S.; Hamel, M. *J. Mater. Chem. C*, **2014**, *Submitted*.

[96] (a) Adadurov, A. F.; Zhmurin, P. N.; Lebedev, V. N.; Kovalenko, V. V. *Nucl. Instr. Methods A* **2010**, *621*, 354-357; (b) Adadurov, A. F.; Zhmurin, P. N.; Lebedev, V. N.; Kovalenko, V. N. *Appl. Radiat. Isot*. **2011**, *69*, 1475-1478.

[97] Bell, C. D.; Bosworth, N. European Patent Application EP0913448, 1999.

[98] (a) Barillon, R.; Bouajila, E.; Douce, L.; Jung, J.-M.; Stuttgé, L. French Patent Application FR2933699, 2008; (b) Mugnier, M. "Nouvelles molécules organiques scintillantes à base de liquides ioniques pour la détection et la discrimination des rayonnements nucléaires", PhD Thesis, University of Strasbourg, France, 2011.

[99] (a) Doty, F. P.; Bauer, C. A.; Skulan, A. J.; Grant, P. G.; Allendorf, M. D. *Adv. Mater*. **2009**, *21*, 95-101; (b) Doty, F. P.; Allendorf, M. D.; Feng, P. L. PCT Patent Application WO2011/060085, 2011.

[100] Perry IV, J. J.; Feng, P. L.; Meek, S. T.; Leong, K.; Doty F. P., Allendorf, M. D. *J. Mater. Chem*. **2012**, *22*, 10235-10248.

[101] Brooks, F. D.; Pringle, R. W.; Funt, B. L. *IRE Trans. Nucl. Sci.* **1960**, *NS-7*, 35-38.

[102] (a) Hamel, M.; Blanc, P.; Dehé-Pittance, C.; Normand, S. French Patent Application FR1352072, 2013; (b) Blanc, P.; Hamel, M.; Rocha, L.; Normand, S.; Pansu, R. *IEEE Nucl. Sci. Symp. Conf. Rec.* **2012**, 1978-1982; (c) Hamel, M.; Blanc, P.; Rocha, L.; Normand, S.; Pansu, R. *Proc. SPIE* **2013**, *8710*, 87101F-1-87101F-7; (d) Blanc, P.; Hamel, M.; Pansu, R. B.; Rocha, L.; Normand, S. *IEEE proceedings of ANIMMA 2013*, **2014**. (e) Blanc, P.; Hamel, M.; Dehé-Pittance, C.; Rocha, L.; Pansu, R. B.; Normand, S. *Nucl. Instr. Methods A* **2014**, *750*, 1-11; (f) Blanc, P.; Hamel, M.; Rocha, L.; Pansu, R. B.; Gobert, F.; Lampre, I.; Normand, S. *IEEE Trans. Nucl. Sci*. **2014**, *Accepted*.

[103] (a) Zaitseva, N.; Carman, L.; Glenn, A.; Hamel, S.; Payne, S. A.; Rupert, B. L. PCT Patent Application WO2012142365, 2012; (b) Zaitseva, N.; Rupert, B. L.; Pawelczak, I.; Glenn, A.; Martinez, H. P.; Carman, L.; Faust, M.; Cherepy, N.; Payne, S. *Nucl. Instr. Methods A* **2012**, *668*, 88-93.

[104] http://www.eljentechnology.com/index.php/products/plastic-scintillators/114-ej-299-33 (last access December 16th, 2013).

[105] (a) Pozzi, S. A.; Bourne, M. M.; Clarke, S. D. *Nucl. Instr. Methods A* **2013**, *723*, 19-23; (b) Nyibule, S.; Henry, E.; Schröder, W. U.; Tõke, J.; Acosta, L.; Auditore, L.; Cardella, G.; Filippo, E. D.; Francalanza, L.; Gìani, S.; Minniti, T.; Morgana, E.; Pagano, E. V.; Pirrone, S.; G. Politi; Quattrocchi, L.; Rizzo, F.; Russotto, P.; Trifirò, A.; Trimarchi, M. *Nucl. Instr. Methods A* **2013**, *728*, 36-39; (c) Cester, D.; Nebbia, G.; Stevanato, L.; Pino, F.; Viesti, G. *Nucl. Instr. Methods A* **2014**, *735*, 202-206.

[106] (a) Zaitseva, N. P.; Carman, M. L.; Faust, M. A.; Glenn, A. M.; Martinez, H. P.; Pawelczak, I. A.; Payne, S. A.; Lewis, K. E. American Patent Application US2013/0299702, 2013; (b) Zaitseva, N.; Glenn, A.; Martinez, H. P.; Carman, L.; Pawełczak, I.; Faust, M.; Payne, S. *Nucl. Instr. Methods A* **2013**, *729*, 747-754.

[107] Hawkes, N. P.; Taylor, G. C. *Nucl. Instr. Methods A* **2013**, *729*, 522-526.

[108] Leinweber, G.; Barry, D. P.; Trbovich, M. J.; Burke, J. A.; Drindak, N. J.; Knox, H. D.; Ballad, R. V *Nucl. Sci. Eng.* **2006**, *154*, 261-279.

[109] Im, H.-J.; Willis, C.; Saengkerdsub, S.; Makote, R.; Pawel, M. D.; Dai, S. *J. Sol-Gel Sci. Techn.* **2004**, *32*, 117-124.

[110] Mugnier, J.; Le Luyer, C.; Garcia Murillo, A. *Proc. SPIE* **2004**, *5250*, 589-596.

[111] Kesanli, B.; Hong, K.; Meyer, K.; Im, H.-J.; Dai, S. *Appl. Phys. Lett.* **2006**, *89*, 214104.

[112] Wallace, S. A.; Stephan, A. C.; Cooper, R.; Im, H.-J.; Dai, S. *Nucl. Instr. Methods A* **2007**, *579*, 184-187.

[113] Koshimizu, M.; Kitajima, H.; Iwai, T.; Asai, K. *Jpn. J. Appl. Phys.* **2008**, *47*, 5717-5719.

[114] Pedroza, G.; de Azevedo, W. M.; Khoury, H. J.; da Silva Jr., E. F. *Appl. Radiat. Isot.* **2002**, *56*, 563-566.

[115] Quaranta, A.; Carturan, S.; Campagnaro, A.; Dalla Palma, M.; Giarola, M.; Daldosso, N.; Maggioni, G.; Mariotto, G. *Thin Solid Films* **2014**, *553*, 188-192.